

Estimating the Electromagnetic Chiral Lagrangian Coefficients

Master of Science Thesis by Anders Pinzke

Thesis advisor: Johan Bijnens

*Department of Theoretical Physics,
Lund University, Lund, Sweden*

Abstract

In the low energy region chiral perturbation theory including virtual photons is used to derive the structure of the generating functional. The work we do is performed within the three flavor framework and reaches up to next-to-leading order. An Euclidian cut-off is introduced to separate the long- and short-distance contributions. The long-distance part is evaluated in the ChPT framework up to $\mathcal{O}(p^4)$. The short-distance part is achieved partly from the work of J. Bijnens and J. Prades [1], through perturbative QCD and factorization. A matching is made and the finite parts of the low-energy constants (LECs) is determined by using already existing data of the QCD LECs up to order p^4 [1], [2], [3].



LUND
UNIVERSITY

Contents

1	Introduction	2
2	Theory	3
2.1	Interpretation of the Lagrangians	3
2.2	Renormalization	4
2.3	Symmetries	6
2.3.1	Spontaneous symmetry breaking	7
2.3.2	The linear sigma model	8
2.3.3	The non-linear sigma-model	10
2.3.4	Goldstone bosons	10
2.4	Chiral perturbation theory	12
2.5	Effective Lagrangians	13
2.5.1	Power counting	13
2.5.2	QCD at low energy	14
2.5.3	QFD at low energies	15
2.5.4	Leading order effective Lagrangian	16
2.5.5	Next-to-leading order effective Lagrangian	16
3	How to determine the EM coefficients	18
4	Result	22
5	Conclusion	32
A	An easy example	34
B	Generating functionals	36
C	External fields	37

1 Introduction

Masses of hadrons have always been a problem to calculate throughout the history of modern particle physics. The problem lies in the fact that the particles are believed to have three different mass contributions; the free quark mass from the Higgs mechanism, the constituent mass and perturbative interactions with γ , W and Z. The last contribution is the one that we are concentrating on. These are called radiative corrections and involve interactions from gauge bosons. For the light mesons that we are going to investigate it is enough to use photon corrections, in an effective low energy model. This model is derived from the Standard Model (SM) which is a relativistic quantum field theory that give rise to the strong interaction described by Quantum Chromo Dynamics (QCD) and the electroweak interaction described by Quantum Flavor Dynamics (QFD). QCD works very well and agrees with experiments at high energies and short distances. It is much more difficult to examine QCD at low energies and long distances. One of the most successful approaches is based on the fact that QCD has a $SU(n_F)_L \times SU(n_F)_R$ chiral symmetry for n_F massless flavors. To get an effective field theory model for low energy, a perturbation of the symmetry above is performed. The perturbation is called chiral perturbation theory (ChPT). This theory can be described by certain fields which correspond to the low energy spectrum of light pseudoscalar mesons, the π , K , and η octet. When \mathcal{L}_{EM} is added to \mathcal{L}_{QCD} the effective Lagrangian for QCD and Electromagnetic (EM) interactions using Weinberg's power counting scheme [4] can be written as:

$$\mathcal{L}_{effective} = \mathcal{L}_2 + \mathcal{L}_4 + \dots = \mathcal{L}_2(C, F_0, B_0) + \sum_{i=1}^{10} L_i O_4^i + \sum_{i=1}^2 H_i \tilde{O}_4^i + \sum_{i=1}^{14} K_i \hat{O}_4^i + \dots \quad (1)$$

where the subscript has been ordered in momenta, mass and electric charge. The O^i 's represent the term in the effective Lagrangian that are connected to the i :th LEC (see Eq. (44)). The lowest order Lagrangian is given by the non-linear sigma model coupled to external fields [5][6]. It contains three free parameters in the chiral limit: the scalar quark condensate B_0 , the pion-decay constant F_0 and the lowest order EM coupling constant C . The leading order expansion $\mathcal{O}(p^2)$ implies tree level diagrams with \mathcal{L}_2 vertices. The next-to-leading order expansion is used to derive the electromagnetic LECs K_i by computing photon loops from the leading order Lagrangian \mathcal{L}_2 and adding contributions from the next-to-leading order Lagrangian \mathcal{L}_4 . Doing the loop calculations will involve all the 29 LECs¹ in Eq. (1) that are connected to the couplings of different vertices in the diagrams, more about this in section 2.5. This is not a problem to us since the purely QCD part connected to B_0 , F_0 , L_i and H_i , have been determined experimentally or theoretically. The constants of order $\mathcal{O}(p^4)$ contain a divergent part and a constant finite part. The divergent part can be isolated with the help of dimensional regularization and \overline{MS} regularization. For the K_i part this was recently done by Urech in [7], but the finite part of the K_i is almost entirely unknown. The goal of this thesis is to determine the K_i as a function of the L_i and H_i .

¹There exist a few more constants up to order $\mathcal{O}(p^4)$, but these are of no importance to us

2 Theory

One of the greatest achievements in physics during the 20th century is the Standard model of particle physics. It revolutionized the view of elementary particles. Protons and neutrons that build up atoms (and electrons, of course) are not considered to be the fundamental particles any more. Instead they consist of point-like particles called quarks. Beside the quarks exist fundamental particles called leptons. In total there are six quarks (u, d, s, c, b, t) and six leptons ($e, \nu_e, \mu, \nu_\mu, \tau, \nu_\tau$) which all matter is composed of. The forces between the fundamental particles are described by the twelve gauge bosons. These particles mediate three forces; the strong-, weak- and the electromagnetic force. Note that the fourth fundamental force (out of the four known) gravity is not included. The weak force which comes from the local $SU(2)$ gauge invariance of the SM Lagrangian and the EM force which originates from the local $U(1)$ gauge symmetry is unified to the electroweak force (described by QED) which is mediated through the four gauge bosons (W^\pm, Z^0, γ). This unified force is based upon the $U(1) \times SU(2)$ symmetry. The strong force comes from the local $SU(3)$ gauge symmetry of the Lagrangian. Due to the non-Abelian² nature of the local $SU(3)$ gauge group, the eight gauge bosons (the gluons) that mediate the strong force, carry "colour" charges such that the QCD Lagrangian incorporates gluon self interaction involving vertices with three and four gluons. This fact complicates things a great deal.

2.1 Interpretation of the Lagrangians

The theory of the SM is written in terms of Lagrangians, which describe the dynamics of a system in a fundamental and well known way. They are scalars in every relevant space and invariant under transformations. In the full field theory, the Lagrangians can be used in a variety of ways. 50 years ago Feynman created a simple method which reduces and simplifies amplitude calculations done in relativistic quantum field theory. This was an important discovery because the amplitude is of great importance since it incorporates the physical picture of a system. Feynman's method is based on diagrams (called Feynman diagrams) which can be used to calculate the amplitude in an efficient way, using so-called Feynman rules. The rules enforce conservation of energy and three-momentum at each vertex, so that the four-momentum for the whole vertex is conserved.

Let us investigate an easy example where, $\pi^0 \rightarrow \gamma\gamma$. The pion, using standard quantum field notation, is written as

$$\pi^0(x) = \int N_{\pi^0}(p)(a_p e^{-ip \cdot x} + a_p^\dagger e^{ip \cdot x}) d^3 p \quad (2)$$

where the creation a^\dagger and annihilation a operators, create and annihilate a pion with momentum p , respectively. The $N_{\pi^0}(p)$ is a numerical factor determined from the Feynman

²Whenever the order of transformations matters, they are called non-Abelian transformations. The non-zero value of a commutator including the Pauli matrices that generate the local $SU(2)$ gauge theory is an example of this.

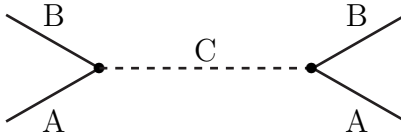
rules. The photon field can also be described in a similar way, but since it is a vector and not a scalar it needs an extra index. A polarization vector ϵ with four components is introduced. The photon field is then represented by

$$A_\mu(x) = \int N_A(q)(\epsilon_\mu a_k e^{-ik \cdot x} + \epsilon_\mu^* a_k^\dagger e^{ik \cdot x}) d^3 q \quad (3)$$

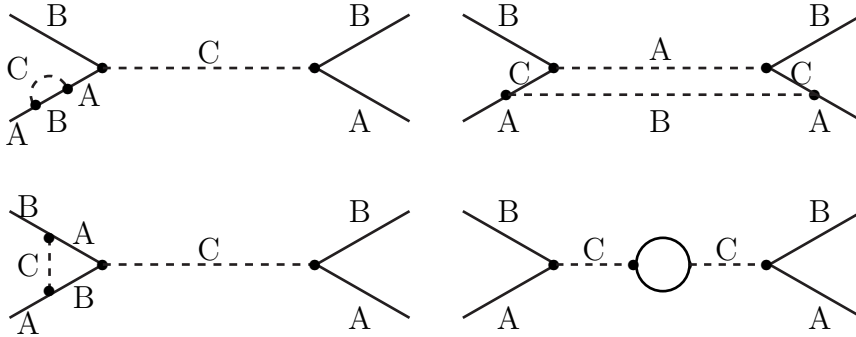
where k is proportional to the momentum q of the created photons. For the $\pi^0 \rightarrow \gamma\gamma$ where one pion is annihilated and two photons are created, the corresponding terms are picked out and used in the Lagrangian to get the Feynman amplitude for the vertex.

2.2 Renormalization

Start by considering lowest order ("tree level") Feynman diagrams, where $A + A \rightarrow B + B$. Assume that the time axis goes from the bottom to the top.



The diagram has two vertices, so the matrix element \mathcal{M} is proportional to the coupling constant squared (g^2). This diagram is not the only one that describes this process, e.g. the four-vertex diagrams below also contribute to the process.



Let us investigate the bottom right diagram containing a loop integral where the four dimensional element could be written as $d^4 q = q^3 dq d\Omega$, where $d\Omega$ represents the angular part. At large q the integrand is essentially $1/q^4$, so the loop integral has the form of:

$$\int^\infty \frac{1}{q^4} q^3 dq = \ln q \Big|^\infty = \infty \quad (4)$$

This integral is logarithmic divergent for large q , which was a problem for a long time. Now there exist systematic methods to get rid of the "problem".

The procedure goes as follows:

(1) *Regularize the integral*: Done by modifying the theory, in such a way that it remains finite and well-defined. This can be done in a couple of different ways which all lead to the

same physical result. In this thesis we will use two different methods, the cut-off procedure and dimensional regularization. The first method mentioned, is the oldest one of the two and it is often used on simpler cases. The other procedure, dimensional regularization, is a powerful method which is based on modifying the dimensionality of the integrals so that they become finite.

(2) *Renormalize*: Where the physical parameters of interest change from the ones introduced by original Feynman rules, to “renormalized” and finite parameters containing extra factors.

(3) *Eliminate the regularizing parameters*: One revert from the regularized theory back to QED, i.e. the original infinities of QED relate the original (bare) particles with the physical particles. This means that the physical observations of the theory expressed in terms of mass and charge are finite as one restores QED.

We will now demonstrate the cut-off procedure to give a feeling about the whole topic. So, the first step is to regularize the integral, where a suitable cut-off procedure is used that removes the infinities for the moment. This renders the integral to a finite value without spoiling the Lorentz invariance. The cut-off is introduced as a “fudge factor” that goes to 1 as the cut-off $\rightarrow \infty$. The nice thing is that the integral can then be calculated and separated into two parts: a finite part, independent of the cut-off, and a term related to the logarithm of the cut-off, which diverges when the cut-off goes to infinity. Now something extraordinary happens, all the divergent cut-off dependent terms appear together with the masses and coupling constants. This means that the physical masses and coupling constants are not the m 's and g 's from the original Feynman rules, instead they are considered to be renormalized ones, i.e

$$m_{\text{physical}} = m + \delta m \qquad g_{\text{physical}} = g + \delta g \qquad (5)$$

In the infinite cut-off limit the delta factors are infinite, but this does not matter, since they are not the measured ones. The measured m_{physical} and g_{physical} are finite, so the m and g in Eq. (5) also diverge, and makes the right side contribution finite. The remaining finite (cut-off independent) terms from the loop integrals, also suffer from the modifications of m and g . But the change in these finite effective masses and coupling constants also depend on the momentum of the particles involved, and therefore they are called running masses and running coupling constants. If all the infinities from higher order diagrams behave in the way described above, we say that the theory is renormalizable. 30 years ago 't Hooft showed that all gauge theories, including QCD and QED, are renormalizable [8].

Another interesting way of viewing renormalization is with the help of a medium. From quantum physics we know that every particle moving through a medium consisting of quantum fluctuations which effect values i.e. charge and mass. To be able to ignore the medium the values of the particles parameters have to be changed to scale-dependent values, and you say that the parameters have been renormalized by the medium.

2.3 Symmetries

Symmetries are very important in particle physics. Whenever there is an invariance there is a corresponding conserved quantity. That is exactly what Noether's theorem says: Symmetry \Leftrightarrow conserved quantity. These conserved quantities and the associated currents create, with the help of group theory the building blocks of the standard model. The SM is full of different symmetries. It is built up out of the three local gauge symmetries $SU(3)_C \times SU(2)_L \times U(1)_Y$, some continuous global symmetries and some discrete symmetries.

The full QCD Lagrangian with the $SU(3)_C$ gauge symmetry can be approximated by a light-flavor Lagrangian, because the scale of interest is $\sim 1\text{GeV}$. So the c, b, and t quark will not be considered, since they are created at a scale over $\sim 1\text{GeV}$. The light-flavor QCD Lagrangian can be written as

$$\mathcal{L}_{QCD} = \sum_{q=u,d,s} i\bar{q}_L \not{D} q_L + i\bar{q}_R \not{D} q_R - m_q(\bar{q}_L q_R + \bar{q}_R q_L) \quad (6)$$

where $q_{L,R} = \frac{1}{2}(1 \pm \gamma_5)q$, $\not{D} = i\gamma^\mu(\partial_\mu - iG_\mu)$ and G_μ the gluon field. The q corresponds to a particular quark state, and its wave function is a product of factors,

$$q = \left(\begin{array}{c} \text{space} \\ \text{factor} \end{array} \right) \times \left(\begin{array}{c} \text{spin} \\ \text{factor} \end{array} \right) \times \left(\begin{array}{c} U(1) \\ \text{factor} \end{array} \right) \times \left(\begin{array}{c} SU(2) \\ \text{factor} \end{array} \right) \times \left(\begin{array}{c} \text{colour} \\ \text{factor} \end{array} \right) \quad (7)$$

where each factor represents some labels, coordinates, or indices. If the masses in the approximated light-flavor Lagrangian are put equal, the Lagrangian gets an extra global symmetry. The symmetry is an $SU(3)$ flavor symmetry (rotation in quark flavor space). In the chiral limit the quark masses $m_q=0$, which implies that $SU(3) \rightarrow SU(3)_L \times SU(3)_R$ since the left and right handed quarks decouple from each other. So $\mathcal{L}_{QCD}^{m=0}$ is invariant under $SU(3)_L \times SU(3)_R \times U(1)_A \times U(1)_V \equiv J$. If we define

$$\Psi = \begin{pmatrix} q_u \\ q_d \\ q_s \end{pmatrix} \quad (8)$$

then the transformations associated with J symmetry correspond to

$$\begin{array}{ll} SU(3)_{V=L+R} & \Psi \rightarrow e^{-i\vec{\theta} \cdot \vec{\lambda}/2} \Psi \\ U(1)_A & \Psi \rightarrow e^{-i\epsilon \gamma_5} \Psi \\ U(1)_V & \Psi \rightarrow e^{-i\epsilon} \Psi \\ SU(3)_L & \Psi_L \rightarrow g_L \Psi_L \\ SU(3)_R & \Psi_R \rightarrow g_R \Psi_R \\ SU(3)_L \times SU(3)_R & \Psi_L + \Psi_R \rightarrow g_L \Psi_L + g_R \Psi_R \quad g_{L,R} \in SU(3)_{L,R} \end{array} \quad (9)$$

where $\vec{\lambda}$ is a vector with the Gell-Mann matrices as its elements. These transformations are later on used to derive the structure of the effective Lagrangians.

A symmetry is usually implemented in one of the two following ways: The Weyl mode and the Goldstone mode. In the Weyl mode the Lagrangian and the vacuum are both invariant under a set of symmetry transformations generated by Q , i.e for the vacuum

$$e^{i\epsilon Q} | 0 \rangle = | 0 \rangle \rightarrow Q | 0 \rangle = 0 \quad (10)$$

where Q is a generator of the symmetry group under consideration. The vacuum $| 0 \rangle$ is unique and defined as the state of the system which

$$\langle 0 | H | 0 \rangle = \min. \quad (11)$$

So the generators Q generate a symmetry i.e. when $[Q, H] = 0$, and $| a \rangle$ and $| a' \rangle$ belong to the same multiplet then $H | a \rangle = E_a | a \rangle$ implies that $H | a' \rangle = E_a | a' \rangle$. This means that a and a' are degenerate states.

In the Goldstone mode the Lagrangian is invariant under the symmetry transformations generated by Q , but $Q | 0 \rangle \neq 0$. The consequence of this will be discussed in detail in the next chapters.

2.3.1 Spontaneous symmetry breaking

In the following we consider an easy example that describes the theory behind spontaneous symmetry breaking. This happens when the symmetry of the Lagrangian is not shared by the groundstate. We will develop this idea and consider the linear sigma- and the non-linear sigma-model, where an effective Lagrangian is derived from the symmetry properties of the theory. Later on we use the same symmetry arguments for the QCD and QFD Lagrangians to determine their form.

Start by consider a Lagrangian with a discrete reflection symmetry, $\phi \rightarrow -\phi$, i.e the ϕ^4 theory Lagrangian

$$\mathcal{L} = \frac{1}{2}(\partial_\mu \phi)^2 - \frac{1}{2}\mu^2 \phi^2 - \frac{\lambda}{4!}\phi^4 \quad (12)$$

where ϕ is a spin-zero scalar field, λ and μ are constants. The field ϕ_0 is the classical minimum of the potential

$$V(\phi) = \frac{1}{2}\mu^2 \phi^2 + \frac{\lambda}{4!}\phi^4 \quad (13)$$

which has two minima for $\mu^2 < 0$,

$$\phi_0 = \pm v = \pm \sqrt{-\frac{6\mu^2}{\lambda}}. \quad (14)$$

The constant v is the vacuum expectation value of ϕ . Now expand around one of the two minima,

$$\phi(x) = v + \sigma(x) \quad (15)$$

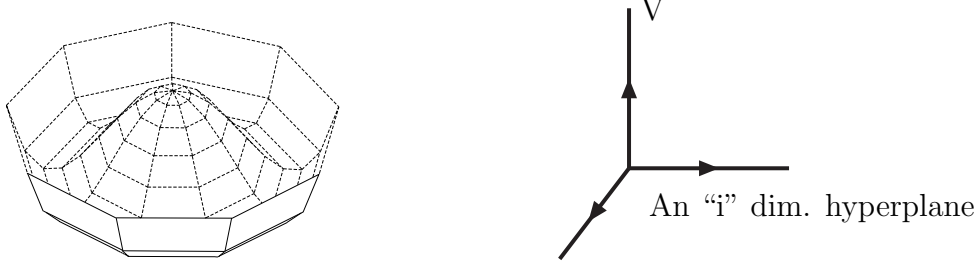


Figure 1: Shows the “Mexican hat potential” in Eq. (18) where the potential energy V is a function of ϕ^i and the plane parallel to V is thought of as an “ i ” dimensional hyperplane.

and rewrite \mathcal{L} in terms of v and σ . Dropping the constant terms, the following \mathcal{L} is obtained

$$\mathcal{L} = \frac{1}{2}(\partial_\mu \sigma)^2 - \frac{1}{2}(-2\mu^2)\sigma^2 - \sqrt{-\frac{\lambda\mu^2}{4!}}\sigma^3 - \frac{\lambda}{4!}\sigma^4 \quad (16)$$

which describes a simple scalar field of mass $\sqrt{-2\mu^2}$, with σ^3 and σ^4 interactions. The reflection symmetry in Eq. (12) is no longer present and you say that it is hidden inside the Lagrangian.

2.3.2 The linear sigma model

A generalization of the discrete symmetry breaking above is the linear sigma model, which has a broken continuous symmetry. This is a phenomenological model for light mesons at low energy. The model consist out of N fields and has a ϕ^4 interaction that is invariant under rotation of the N fields. The Lagrangian is

$$\mathcal{L} = \frac{1}{2}(\partial_\mu \phi^i)^2 - \frac{1}{2}\mu^2(\phi^i)^2 - \frac{\lambda}{4}((\phi^i)^2)^2 \quad (17)$$

where $i=1, \dots, N$ and is summed over. The last two terms form the potential and are often written as

$$V(\phi^i) = \frac{1}{2}\mu^2(\phi^i)^2 + \frac{\lambda}{4}((\phi^i)^2)^2. \quad (18)$$

The Lagrangian in Eq. (17) is invariant under the symmetry transformation

$$\phi^i \rightarrow R^{ij}\phi^j \quad (19)$$

for an $N \times N$ orthogonal matrix R which imply that \mathcal{L} has an $O(N)$ symmetry. The potential V has a local maximum at $\phi^i = 0$ for $\mu^2 < 0$. The minimum (ground state) can

be found through $\frac{\partial V}{\partial \phi^i}$ and thought of as a multidimensional circle. Excitations in the N :th direction (radial direction) require a shift away from the minimum, whilst an excitation along the circle, where the potential is flat, corresponds to the other $N - 1$ directions. Here an intuitive physical picture can be seen, and as will be seen later, the excitation in the radial direction corresponds to a massive particle and an excitation along the flat potential gives rise to massless particles. The chosen minimum of the potential, ϕ_0 , can be written in the following way:

$$\begin{aligned}\phi_0^i(x) &= 0 & i &= 1, \dots, N - 1 \\ \phi_0^i(x) &= v & i &= N\end{aligned}\quad (20)$$

When a perturbation expansion is performed, the fluctuations around ϕ_0 have to be considered instead of the fluctuations around $\phi = 0$. This means that

$$\phi^i(x) = (\varphi^k(x), v + \tilde{\sigma}(x)) \quad k = 1, \dots, N - 1 \quad (21)$$

where $\varphi^k(x)$ are the light meson fields and v the vacuum expectation value. The original $O(N)$ symmetry is then hidden (broken) and the remaining symmetry is $O(N - 1)$, which rotate the $\varphi^k(x)$ among themselves. Now Eq. (17) can be rewritten by replacing the old ϕ^i with the new one in Eq. (21). The following result is then obtained

$$\begin{aligned}\mathcal{L} &= \frac{1}{2}(\partial_\mu \tilde{\varphi}^k)^2 + \frac{1}{2}(\partial_\mu \tilde{\sigma})^2 - \frac{1}{2}(-2\mu^2)\tilde{\sigma}^2 - \sqrt{-\lambda\mu^2}\tilde{\sigma}^3 - \sqrt{-\lambda\mu^2}(\varphi^k)^2\tilde{\sigma} \\ &\quad - \frac{\lambda}{4}\tilde{\sigma}^4 - \frac{\lambda}{2}(\varphi^k)^2\tilde{\sigma}^2 - \frac{\lambda}{4}((\varphi^k)^2)^2\end{aligned}\quad (22)$$

where $N - 1$ massless meson fields and one massive sigma field have appeared.

If $N=4$ ³ an $O(4)$ symmetry is achieved, which means that

$$\phi = \begin{pmatrix} \sigma \\ \pi_1 \\ \pi_2 \\ \pi_3 \end{pmatrix} \rightarrow \begin{pmatrix} \sigma' \\ \pi'_1 \\ \pi'_2 \\ \pi'_3 \end{pmatrix} = O \begin{pmatrix} \sigma \\ \pi_1 \\ \pi_2 \\ \pi_3 \end{pmatrix} \quad (23)$$

where O is an orthogonal 4×4 matrix that rotate the matrix ϕ . This means that the four primed fields are linear combinations of the unprimed fields, and that the fields transform linearly. If $\sigma = v + \tilde{\sigma}$ is considered, where the sigma field is a scalar field and has a non-vanishing vacuum expectation value, then Eq. (22) can be rewritten as

$$\mathcal{L} = \frac{1}{2}\partial_\mu \tilde{\varphi} \cdot \partial^\mu \tilde{\varphi} + \frac{1}{2}\partial_\mu \sigma \partial^\mu \sigma - \frac{\mu^2}{2}(\sigma^2 + \tilde{\varphi}^2) - \frac{\lambda}{4}(\sigma^2 + \tilde{\varphi}^2)^2 \quad (24)$$

Using a representation called the exponential representation

$$S \equiv \sqrt{\sigma^2 + \tilde{\varphi}^2} - v, \quad U \equiv \exp(i\vec{\tau} \cdot \vec{\varphi}'/v). \quad (25)$$

³ $N=4$ is useful because $O(4) \cong SU(2) \times SU(2)$ which means that the exponential representation with the Pauli matrices can be used.

The resulting Lagrangian can be written in the form

$$\mathcal{L} = \frac{1}{2}((\partial_\mu S)^2 - 2\mu^2 S^2) - \lambda v S^3 - \frac{\lambda}{4} S^4 + \frac{(v + S)^2}{4} \langle \partial_\mu U \partial^\mu U^\dagger \rangle \quad (26)$$

where $\langle \dots \rangle$ is the trace in flavor space. Since we have done the switch $\phi \rightarrow U$, using local group arguments⁴, the linear transformation is not valid anymore. The matrix U is invariant under $SU(2)_L \times SU(2)_R$, but this is a non-linear transformation, which can be seen explicitly when we Taylor expand

$$U \simeq 1 + \frac{1}{v} \vec{\tau} \cdot \vec{\varphi}' - \frac{(\vec{\tau} \cdot \vec{\varphi}')^2}{v^2} + \dots \quad (27)$$

and use that $U \rightarrow g_L U g_R^\dagger \Rightarrow \vec{\tau} \cdot \vec{\varphi}' \rightarrow g_L \vec{\tau} \cdot \vec{\varphi}' g_R^\dagger + \dots$. So the Lagrangian in Eq. (26) can be thought of as the non-linear representation of the linear sigma model.

2.3.3 The non-linear sigma-model

When physics is studied at a specific energy scale only particles that can be created inside this energy scale have to be considered. The heavy fields do then not turn up explicitly, but can be seen through virtual effects. When an effective \mathcal{L} (see chapter 2.5) is used at low energies the heavy fields do not have to be included, but the virtual effects are included via LECs connected to only light fields. There is a theorem called the decoupling theorem that says that all effects from heavy fields will reveal themselves through renormalization of coupling constants or they can be ignored because of the heavy mass suppression. At low energy, Eq. (26) can be expanded to a very interesting form. By only considering lowest order $\varphi' \varphi'$ -interactions the only interesting term is the one without the field S , so all diagrams with S interactions and S propagators are neglected. The non-linear sigma model is achieved when $S \rightarrow 0$, which implies that

$$\mathcal{L} = \frac{v^2}{4} \langle \partial_\mu U \partial^\mu U^\dagger \rangle. \quad (28)$$

This is of great importance as we will see later on. Without external fields and EM interactions this term is the only term of $\mathcal{O}(p^2)$.

2.3.4 Goldstone bosons

That massless particles show up when a continuous symmetry is broken, is a consequence from Goldstone's theorem[9]. The theorem says that for every spontaneous broken symmetry, the theory must contain a massless particle. So the result from an $O(N)$ -symmetric theory as for the linear sigma model with $N - 1$ broken symmetries, is $N - 1$ massless particles. The massless particles are called Goldstone bosons (GB).

⁴ $\vec{\varphi}'$ is determined from $\sigma + i\vec{\tau} \cdot \vec{\varphi} = (S + v)U$.

As I mentioned before the Lagrangian is invariant, but $Q | 0 \rangle \neq 0$ for a number of generators. This implies that in the vacuum there are operators that form states of particles, denoted $|\pi^a(k)\rangle$. This fact will be used later on when we show that the non-linear sigma model is equivalent with \mathcal{L}_{QCD} .

In the earlier chapters the symmetry of the QCD Lagrangian was discussed and in the chiral limit a $SU(3)_L \times SU(3)_R \times U(1)_A \times U(1)_V$ symmetry was achieved. If only the two lightest quarks had been considered then the QCD Lagrangian would have a $SU(2)_L \times SU(2)_R \times U(1)_A \times U(1)_V$. The first two groups corresponds to $SO(4)$ (true under Lie algebra). The interesting part is that since $SO(4) \rightarrow SO(3)$ under spontaneous symmetry breaking (where $SO(3)$ corresponds to $SU(2)$ under similar group argument as above)⁵ $SU(2)_L \times SU(2)_R \rightarrow SU(2)_{V=L+R}$, where $SU(2)_{V=L+R}$ is a subgroup of the chiral symmetry. Using the same arguments as above $G \equiv SU(3)_L \times SU(3)_R \rightarrow SU(3)_{V=L+R} \equiv H$. Since the global axial part of \mathcal{L}_{QCD} in the chiral limit is broken and the fact that we are working in $SU(3)$, eight⁶ pseudoscalar Goldstone bosons (GB) appear as a consequence of Goldstone's theorem.

The massless particles showing up form the light meson octet containing: $\pi^\pm, \pi^0, K^\pm, K^0, \bar{K}^0, \eta$. The reason for this is that the light particles have the correct quantum numbers to be associated with the generators of the coset space G/H , which parameterize the GB. Since the GB are massless in this theory, their masses have to be introduced in a different way. It can be added to \mathcal{L}_{QCD} , but this will break the perfect chiral symmetries. The adding of the mass terms to the QCD Lagrangian is analogous to adding a $a\Phi$ term to the potential in Eq. (18). Using a perturbative ansatz, one obtains massive GB, where the squared masses are proportional to the breaking parameter a . Since the masses of the three light quarks are small compared to the breaking scale of chiral symmetries ($\sim 1GeV$)⁷, the explicit adding of the mass can be treated as a small perturbation. The fact that the pseudoscalar-meson masses are much smaller than the typical hadronic scale reinforces this assumption.

One more interesting feature of this is that the non-vanishing masses of the light pseudoscalars in the "real" world, are related to the explicit symmetry breaking in QCD due to the light quark masses which are believed to acquire their mass from the Higgs mechanism.

⁵ $SU(2)$ is locally identical to the rotations in three dimensions, which form the group $SO(3)$, but they differ globally i.e. for rotations that are not infinitesimally small. The two groups have the same Lie algebra, i.e. their generators have the same commutator relations

⁶The number of GB is determined by the symmetry properties of the groups. The G group denote the symmetry group of the Lagrangian, with n_G generators. The H subgroup, that leaves the vacuum after spontaneous symmetry breaking invariant, has n_H generators. Every generator that does not annihilate the vacuum creates one massless GB, i.e. the total number of GB is $n_G - n_H$. In our case $n_G = 16$ and $n_H = 8$, which means that eight Goldstone bosons appear.

⁷Around this energy the spin-one states (ρ, K^*, ϕ) can be created with the same quark content as the light meson octet. The spin-one particles can not be GB, since GB have spin zero if Lorentz invariance is a good symmetry.

2.4 Chiral perturbation theory

Chiral perturbation theory (ChPT) is based upon the following two basic assumptions:

1. The spontaneous breakdown of the $SU(3)_L \times SU(3)_R$ symmetry to $SU(3)_V$ for the QCD Lagrangian in the chiral limit.
2. Close to the chiral limit the mass terms of the light quarks can be treated as small perturbations.

It is very useful for strong interactions in the low energy sector. As seen in previous chapters the symmetry of the QCD Lagrangian is spontaneously broken to $SU(3)_V \times U(1)_V$ which introduces eight massless Goldstone bosons in the form of the (π, K, η) octet. Since $U(1)_V$ corresponds to the baryon number it plays no further role in low energy meson physics.

When the quark masses are added to \mathcal{L}_{QCD} , the pseudoscalar mesons acquire mass through an explicit chiral symmetry breaking. The mass is added through a chiral invariant coupling of the mesons to the scalar and pseudoscalar external currents (see appendix C) s and p , respectively,

$$\chi = 2B_0(s + ip) \rightarrow 2B_0 g_R(s + ip) g_L^\dagger \quad (29)$$

where $g_{L,R} \in SU(3)_{L,R}$, B_0 is related to the quark condensate $\langle 0 | \bar{u}u | 0 \rangle = -F_0^2 B_0 [1 + O(m_q)]$, p is a 3×3 matrix containing eight pseudoscalar external fields related to the $\bar{q}\gamma_5 q$ current. The scalar external currents includes the masses for the three light quarks,

$$s = \mathcal{M} + \dots = \begin{pmatrix} m_u & & \\ & m_d & \\ & & m_s \end{pmatrix} + \dots \quad (30)$$

and are related to the $\bar{q}q$ current. To get rid of the part of the external current s which is of no importance to us, put it exactly equal to the mass matrix. By doing this $\chi \not\rightarrow g_L \chi g_R^\dagger$, so the chiral symmetry breaks, but the quark masses are small compared to the constituent mass, so this can be treated as a perturbation. And since the creation of the GB is based upon the $SU(3)_L \times SU(3)_R$ symmetry which is broken by the perturbative mass, the GB change to pseudo-GB.

ChPT is a non-renormalizable theory, because of the ultraviolet divergences produced by the loops. For a non-renormalizable theory infinite numbers of counterterms have to be added to make it finite. The problem can be avoided by using effective quantum field theory (see effective Lagrangian chapter), which indicate that the energy region of interest is below a certain cut-off parameter Λ , and then the number of counterterms needed at each level of expansion is finite. At increasing expansion powers, the number of needed counterterms increases drastically. At very low energies, the contributions from higher orders are small, that is why only terms up to $\mathcal{O}(p^4)$ are considered here, see Eq.(1). The finite parts for each power contains a finite coupling constant and it is some of those constants that are going to be determined in this thesis. The problem is that they cannot be calculated directly from the QCD and QFD Lagrangians.

2.5 Effective Lagrangians

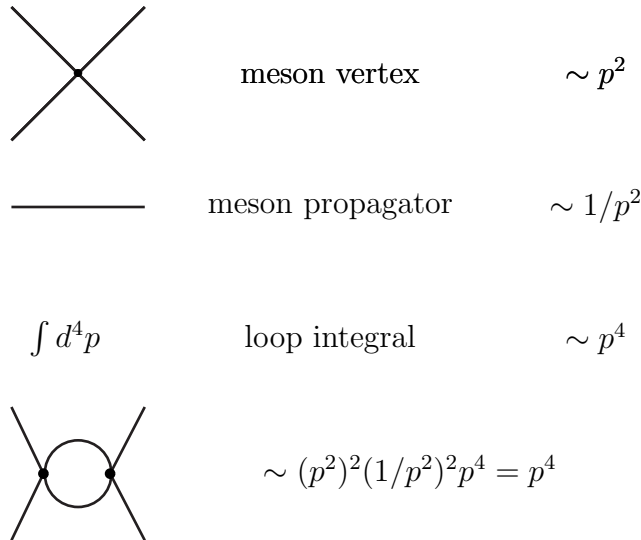
The reason why an effective Lagrangian is used is that at high energies QCD is perturbative, i.e it can be expanded in terms of α_s , which is small for large energies. At low energies the theory is highly non-perturbative since α_s is large and we therefore need to use effective Lagrangian techniques. When effective Lagrangians are used instead of the original Lagrangians, they correspond to the same symmetries but generate different Feynman diagrams.

Most theories in physics are an approximation to the real world. The perturbative treatment is a common and well known method. For the task of this thesis a perturbative theory is needed. The problem can be solved if a light pseudoscalar meson representation is used. The representation is not expanded in terms of α_s , but instead in terms of quark masses and momenta. This is known as chiral expansion.

For low enough energies only a few relevant degrees of freedom are needed to describe the theory. The non-relevant d.o.f can be integrated out and encoded into the LECs, just as for the non-linear sigma model. The effective low energy action that is described by a number of relevant and non-relevant fields, can be written in the form of external fields in the GB low energy theory. The earlier mentioned Lagrangian is then modified, and the external fields can be included in a chiral invariant way.

2.5.1 Power counting

Power counting is a very useful way to organize the powers in the chiral expansion. The ordering in the context of Feynman rules is that, derivatives generate four momenta and the quark mass terms have the same dimension as two derivatives. So when we are on-shell $m_{meson}^2 = p^2$, but when we are off-shell e^2 has the same counting as the four momenta squared. The external photon fields are of order p since they occur together with a momentum in the covariant derivative. An illustrative example can be seen below:



In the figure above, the loop diagram is of $\mathcal{O}(p^4)$ and is generated by tree level diagrams from \mathcal{L}_2 . The loop integrals generate divergences which can be canceled by adding tree diagrams, from the \mathcal{L}_4 terms. The counterterms needed to cancel the divergences created by the loop diagrams of $\mathcal{O}(p^n)$ comes from the LECs of the same order, which implies two things. First the good thing which is that the loop integral divergences are canceled order by order. The other thing is that the number of coefficients needed to describe the theory increases dramatically for increasing orders, which makes an expansion to higher orders almost impossible.

For $\pi\pi$ scattering in pure QCD, an infinite number of diagrams have to be considered since they are equally important. If instead an effective theory is considered, the diagrams can be divided into groups of different powers of p^2 . For low energy, only few powers of p^2 have to be considered. The physical picture can then be described by a small number of diagrams, which is a good approximation of QCD for low energy.

2.5.2 QCD at low energy

At low energies quarks do not behave like free quarks, instead they behave like asymptotic light meson fields. The effective theory of QCD is formulated in this way. It can be expanded in a series of infinite numbers of derivative terms, i.e

$$\mathcal{L}_{eff} = \mathcal{L}_2 + \mathcal{L}_4 + \mathcal{L}_6 + \dots \quad (31)$$

From the properties of the GB and the symmetry of QCD⁸, the easiest form of the leading order terms is

$$\mathcal{L}_2^{QCD} = \frac{F_0^2}{4} \langle \partial^\mu U^\dagger \partial_\mu U + 2B_0 \mathcal{M}(U^\dagger + U) \rangle \quad (32)$$

where \mathcal{M} is the mass matrix in Eq. (30). U contain the eight pseudoscalar meson fields and has the following properties:

$$\begin{aligned} UU^\dagger &= \mathbf{1}, & \det U &= 1 \\ U &= \exp\left(\frac{i\Phi}{F_0}\right), & \Phi &= \sum_{a=1}^8 \lambda_a \varphi_a, \end{aligned} \quad (33)$$

where

$$\Phi = \sqrt{2} \begin{pmatrix} \frac{\pi^0}{\sqrt{2}} + \frac{\eta_8}{\sqrt{6}} & \pi^+ & K^+ \\ \pi^- & -\frac{\pi^0}{\sqrt{2}} + \frac{\eta_8}{\sqrt{6}} & K^0 \\ K^- & \bar{K}^0 & -\frac{2\eta_8}{\sqrt{6}} \end{pmatrix}. \quad (34)$$

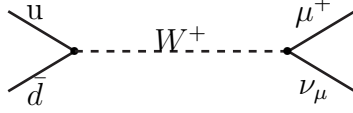
The observant reader can see that in the chiral limit, the vacuum expectation value v in the non-linear sigma model in Eq. (28) can be put equal to the pion decay coupling F_0 . This

⁸With this I mean by adding local contributions to the external fields the transformations associated with the J symmetry in Eq. (9) implies certain invariances, which are used to derive the structure of the effective Lagrangians. All this follows from Gasser & Leutwyler [6].

coupling constant is defined from the differentiation of the lowest order classical action $S_2 = \int d^4x \mathcal{L}_\epsilon$ with respect to external axial fields in the chiral limit, i.e.

$$\langle 0 | \frac{\delta S_2}{\delta a_\mu} | \pi^+(p) \rangle = \langle 0 | \bar{d} \gamma^\mu \gamma_5 u | \pi^+(p) \rangle = i\sqrt{2}F_0 p^\mu. \quad (35)$$

We compare this with the pion decay constant which is derived as follows: The decay of a π^+ into two leptons via a weak interaction can be described by the tree level diagram



Written in terms of matrix elements, this corresponds to

$$\langle W^+ | \mathcal{L} | \pi^+(p) \rangle \sim \langle W^+ | \bar{W}_\mu^+ | 0 \rangle \langle 0 | \bar{d} \gamma^\mu \gamma_5 u | \pi^+(p) \rangle \quad (36)$$

The pion decay constant is then defined to be the second term on the right side. When the amplitude is calculated the following is achieved

$$i\sqrt{2}F_\pi p^\mu = \langle 0 | \bar{d} \gamma^\mu \gamma_5 u | \pi^+(p) \rangle \quad (37)$$

and the identification $F_\pi = F_0$ can be made.

2.5.3 QFD at low energies

The electromagnetic virtual interactions of order e^2 between pseudo-GB to the leading order in the chiral expansion which was first derived by R. Dashen [10] and is described by the effective Lagrangian

$$\mathcal{L}_2^{EM} = e^2 C_1 \langle Q^2 \rangle + e^2 C \langle QUQU^\dagger \rangle \quad (38)$$

which is created from the symmetry properties for an effective low energy QFD theory. To ensure the chiral $SU(3)_L \times SU(3)_R$ symmetry in Eq. (38), the local spurions⁹

$$\begin{aligned} Q_L &\rightarrow g_L Q g_L^\dagger \\ Q_R &\rightarrow g_R Q g_R^\dagger \end{aligned} \quad (39)$$

are introduced instead of the charge matrix Q . The first term in Eq. (38) is a constant and will not be considered. So the resulting Lagrangian is

$$\mathcal{L}_2^{EM} = e^2 C \langle Q_L U Q_R U^\dagger \rangle. \quad (40)$$

The two spurions, Q_L and Q_R , are different matrices. Since the photon couples identically to the left respectively right, it can not distinguish between the two Q matrices and for that reason we put them equal in our effective Lagrangians.

⁹Spurions are dummy fields that are added to the Lagrangian to make it a singlet under the chiral group.

2.5.4 Leading order effective Lagrangian

The effective Lagrangian of QCD including EM effects to leading order is in the mesonic sector

$$\mathcal{L}_2 = -\frac{1}{4}F_{\mu\nu}F^{\mu\nu} - \frac{1}{2(1-\xi)}(\partial_\mu A^\mu)^2 + \frac{1}{4}F_0^2\langle D^\mu U^\dagger D_\mu U + \chi U^\dagger + \chi^\dagger U \rangle + e^2 C \langle QUQU^\dagger \rangle \quad (41)$$

where, the two first terms describe the kinetic energy and the gauge fixing term¹⁰ for the virtual photons. When one takes the inverse of the two terms it will result in the photon propagator that we later on use to calculate the photon loops. $F_{\mu\nu} = \partial_\mu A_\nu - \partial_\nu A_\mu$ is the electromagnetic field strength tensor of the photon field A_μ and ξ is a gauge fixing term. The covariant derivative in Eq. (41) conserves the local gauge symmetries since it includes the couplings to the photon field A_μ , the external vector v_μ and axial-vector currents a_μ ,

$$D_\mu U = \partial_\mu - i(v_\mu + a_\mu)U + iU(v_\mu - a_\mu) = \partial_\mu - ir_\mu U + iUl_\mu \quad (42)$$

where $v_\mu = \frac{\lambda^a}{2}v_\mu^a = e^2QA_\mu + \tilde{v}_\mu$, and $a_\mu = \frac{\lambda^a}{2}a_\mu^a$ is a 3×3 matrix associated to the quark current $\bar{q}\gamma_\mu\gamma^5\lambda^a q$. \tilde{v}_μ is associated with $\bar{q}\gamma_\mu\lambda^a q$, but this current is not of interest to us. The Q matrix in Eq. (41) is the charge matrix for the u, d, and s quark,

$$Q = \frac{1}{3} \begin{pmatrix} 2 & & \\ & -1 & \\ & & -1 \end{pmatrix}. \quad (43)$$

As we have seen above, the lowest order Lagrangian, \mathcal{L}_2 , is given by the non-linear sigma model coupled to external fields. When calculating a process using only tree level diagrams of \mathcal{L}_2 , one represents the results of current algebra. The tree level diagrams can be put together to one-loops diagrams where we have an emission and absorption of a photon in the pseudo-GB theory, generated by the two-point function (Fig. 2), which include the vertices $\gamma P^+ P^-$ and $\gamma\gamma P^+ P^-$ incorporated in Eq. (41). A calculation of one-loop diagrams with \mathcal{L}_2 vertices, leads to divergences as I mentioned before. Due to Weinberg's counting these infinities are of $\mathcal{O}(p^4)$ and can be canceled through renormalization by next-to-leading order Lagrangian at $\mathcal{O}(p^4)$.

2.5.5 Next-to-leading order effective Lagrangian

The Lagrangian in Eq. (41) is only the first term in the infinite chiral expansion series. Here we introduce the second term in the expansion. The first part of it is of order p^4 and for the three light quark approximation in the pure strong sector ($Q = 0$), it was first written down by Gasser and Leutwyler [6], while the EM part of order $p^2 e^2$ was first derived by Urech [7].

¹⁰The main reason why the gauge fixing term is introduced is to avoid singularities when the photon mass equals zero.



Figure 2: The two first types of one-loop contributions from Eq. (41). The crosses are external pseudoscalar currents and the wiggly line is the virtual photon. The full lines are pseudoscalars.

The \mathcal{L}_4 Lagrangian contains all allowed operators that transform linearly and are invariant under the correct symmetries of QCD and QFD. It is given by:

$$\begin{aligned}
\mathcal{L}_4 = \mathcal{L}_4^{QCD} + \mathcal{L}_4^{EM} = & L_1 \langle D_\mu U D^\mu U^\dagger \rangle^2 + L_2 \langle D_\mu U D^\nu U^\dagger \rangle^2 + L_3 \langle D_\mu U D^\mu U^\dagger D_\nu U D^\nu U^\dagger \rangle \\
& + L_4 \langle D_\mu U D^\mu U^\dagger \rangle \langle \chi U^\dagger + U \chi^\dagger \rangle + L_5 \langle (D_\mu U D^\mu U^\dagger) (\chi U^\dagger + U \chi^\dagger) \rangle \\
& + L_6 \langle \chi U^\dagger + U \chi^\dagger \rangle^2 + L_7 \langle \chi U^\dagger - U \chi^\dagger \rangle^2 + L_8 \langle \chi U^\dagger \chi U^\dagger + U \chi^\dagger U \chi^\dagger \rangle \\
& + i L_9 \langle R_{\mu\nu} D^\mu U D^\nu U^\dagger + L_{\mu\nu} D^\mu U^\dagger D^\nu U \rangle + L_{10} \langle R_{\mu\nu} U L^{\mu\nu} U^\dagger \rangle \\
& + H_1 \langle R_{\mu\nu} R^{\mu\nu} + L_{\mu\nu} L^{\mu\nu} \rangle + H_2 \langle \chi^\dagger \chi \rangle \\
& + e^2 F_0^2 K_1 \langle D^\mu U^\dagger D_\mu U \rangle \langle Q^2 \rangle + e^2 F_0^2 K_2 \langle D^\mu U^\dagger D_\mu U \rangle \langle QUQU^\dagger \rangle \\
& + e^2 F_0^2 K_3 \langle QU^\dagger D^\mu U Q D_\mu U^\dagger U + Q U D^\mu U^\dagger Q D_\mu U U^\dagger \rangle \\
& + e^2 F_0^2 K_4 \langle QU^\dagger D^\mu U Q D_\mu U U^\dagger \rangle \\
& + e^2 F_0^2 K_5 \langle (D^\mu U D_\mu U^\dagger + D^\mu U^\dagger D_\mu U) Q^2 \rangle \\
& + e^2 F_0^2 K_6 \langle D^\mu U^\dagger D_\mu U QU^\dagger QU + D^\mu U D_\mu U^\dagger QUQU^\dagger \rangle \\
& + e^2 F_0^2 K_7 \langle \chi^\dagger U + U^\dagger \chi \rangle \langle Q^2 \rangle + e^2 F_0^2 K_8 \langle \chi^\dagger U + U^\dagger \chi \rangle \langle QUQU^\dagger \rangle \\
& + e^2 F_0^2 K_9 \langle (\chi^\dagger U + U^\dagger \chi + \chi U^\dagger + U \chi^\dagger) Q^2 \rangle \\
& + e^2 F_0^2 K_{10} \langle (\chi^\dagger U + U^\dagger \chi) QU^\dagger QU + (\chi U^\dagger + U \chi^\dagger) QUQU^\dagger \rangle \\
& + e^2 F_0^2 K_{11} \langle (\chi^\dagger U - U^\dagger \chi) QU^\dagger QU + (\chi U^\dagger - U \chi^\dagger) QUQU^\dagger \rangle \\
& + e^2 F_0^2 K_{12} \langle U D^\mu U^\dagger [\nabla_\mu^R Q, Q] + U^\dagger D^\mu U [\nabla_\mu^L Q, Q] \rangle \\
& + e^2 F_0^2 K_{13} \langle \nabla_\mu^R Q U \nabla_\mu^L Q U^\dagger \rangle + e^2 F_0^2 K_{14} \langle \nabla_\mu^R Q \nabla_\mu^R Q + \nabla_\mu^L Q \nabla_\mu^L Q \rangle \quad (44)
\end{aligned}$$

where the covariant derivatives $\nabla_\mu^{L(R)}$ are defined as

$$\nabla_\mu^{L(R)} Q = \partial_\mu Q - i[v_\mu - (+)a_\mu, Q] \quad (45)$$

and the L and R field strengths are

$$\begin{aligned} L^{\mu\nu} &= \partial^\mu l^\nu - \partial^\nu l^\mu - i[l^\mu, l^\nu] \\ R^{\mu\nu} &= \partial^\mu r^\nu - \partial^\nu r^\mu - i[r^\mu, r^\nu]. \end{aligned} \quad (46)$$

The coupling constants L_i , H_i and K_i are defined as

$$\begin{aligned} L_i &= \Gamma_i \lambda + L_i^r(\mu), \\ H_i &= \Delta_i \lambda + H_i^r(\mu), \\ K_i &= \Sigma_i \lambda + K_i^r(\mu), \end{aligned} \quad (47)$$

where the Γ_i and Δ_i constants are determined by Gasser and Leutwyler in [5] and the Σ_i constants by Urech in [7]. λ is the divergent part of the coupling constants and can be determined through dimensional regularization and \overline{MS} regularization. The $L_i^r(\mu)$, $H_i^r(\mu)$ and $K_i^r(\mu)$ are, respectively, finite parts, which we are going to determine. These coefficients are renormalized and depend on the arbitrary renormalization scale μ .

3 How to determine the EM coefficients

The main idea behind the calculations of the K_i s is based on the investigation of a single two-point function using two different methods, and comparing them in the end. On the RHS we use pure ChPT to $\mathcal{O}(p^4)$, describing both QCD and QFD with internal photons. The amplitudes for the relevant Feynman diagrams on this side are generated by $\mathcal{L}_{eff} = \mathcal{L}_2 + \mathcal{L}_4 + \dots$. On the other side, the LHS, we use external photons coupled to an effective Lagrangian with a QCD symmetry, $\mathcal{L}_{eff}^{QCD} = \mathcal{L}_2^{QCD} + \mathcal{L}_4^{QCD} + \dots$.

First a summary of the plan:

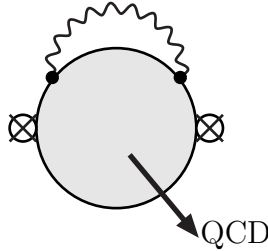
- Investigate the Lagrangians \mathcal{L}_2 in Eq. (41) and \mathcal{L}_4 in Eq. (44).
- Expand the U matrix and plug in the matrices in Eq. (34), Eq. (42) and Eq. (43).
- Consider the relevant Feynman diagrams.
- Integrate over the momenta.
- Calculate the amplitudes for the relevant processes.
- Compare the different amplitudes generated by $\mathcal{L}_{eff}^{QCD} = \mathcal{L}_2^{QCD} + \mathcal{L}_4^{QCD} + \dots$ on the left hand side (LHS) with $\mathcal{L}_{eff} = \mathcal{L}_2 + \mathcal{L}_4 + \dots$ on the right hand side (RHS).

The main result in the chapters before is the Lagrangian in Eq. (44) of $\mathcal{O}(p^4)$ (where the $e^2 p^2$ tree-level contribution from Eq. (44) also is of this order). By expanding U in terms of the meson matrix Φ and plugging in all the matrices into the Lagrangian, the terms that build up the Feynman diagrams are achieved. To handle all the terms by hand is a very

bothersome task, since there are so many of them. Instead we use the computer program Form to calculate the terms. They are carefully investigated and divided up into certain Feynman diagrams, e.g $\pi\pi$ interaction with different kinds of loop diagrams. The terms from the Lagrangian are translated according to the Feynman rules and the amplitude for each diagram is calculated. This is easier said than done, since the diagrams with a loop contain a loop integral over every relevant four-momenta. These integrals are calculated with different methods, depending if it is on the RHS or the LHS. The reason for this is that the two sides are related to different theories describing the same two-point function (appendix B).

We will now investigate the two sides separately.

Left hand side, (LHS) Here we use a Lagrangian with a QCD symmetry including external virtual photons. There exist no divergences except the ones that can be absorbed with renormalization into m_q , α_s and α_{EM} . The following picture illustrates the process



where the figure describes a two-point function, with a virtual photon connected to it. The "bubble" generated by the Green function can be thought of as a propagator describing a process from one side to another.

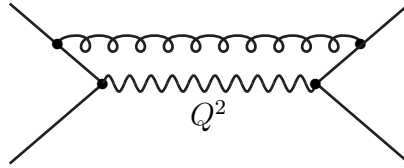
The vital point is that since we are dealing with virtual photons an integration over the whole four-momentum space has to be performed. This is going to give us divergences, which are absorbed as I mentioned before. The integrals over the momentum are divided up into two parts with the help of a cut-off (not the same cut-off used in the renormalization chapter) which respectively is determined by a different method. The two parts are separated into a long-distance (LD) and a short-distance (SD) contribution, with the help an euclidian cut-off Λ . The cut-off also works as a matching variable where a plateau in Λ indicates matching. After passing from Minkowski space to Euclidian space with the help of a Wick rotation¹¹, the integrals can be written in the following form

$$\int_0^\infty dr_E = \int_0^\Lambda dr_E + \int_\Lambda^\infty dr_E. \quad (48)$$

where r_E is the momentum. The first integral, the LD part, is evaluated using ChPT to $\mathcal{O}(p^4)$ which we will explain more in a moment. The second integral, called the SD part, is calculated with perturbative QCD.

¹¹This means that the zeroth component of the four-momenta, $p^0 = ip_E^0$, where p^0 is in the Minkowski space and p_E^0 in the euclidian space

SD We evaluate the photons which have a momentum larger than Λ . This is done through an expansion in powers of $1/\Lambda$, where contributions up to next to leading order are considered. The essence of the physical picture can be illustrated through a simple one-loop diagram.



We use large photon momenta, so that the Q^2 is big. This means that a gluon or a quark has to be included to run back with the momentum Q , otherwise the diagram is heavily suppressed. The suppression comes from the fact that if only “one-way” diagrams are considered, where the energy flows in one direction then the creation of the final hadron is suppressed since the quarks carry too much energy.

In the calculations of the SD part we consider four types of different contributions, each associated with one type of diagram and expanded to order $1/\Lambda^2$.

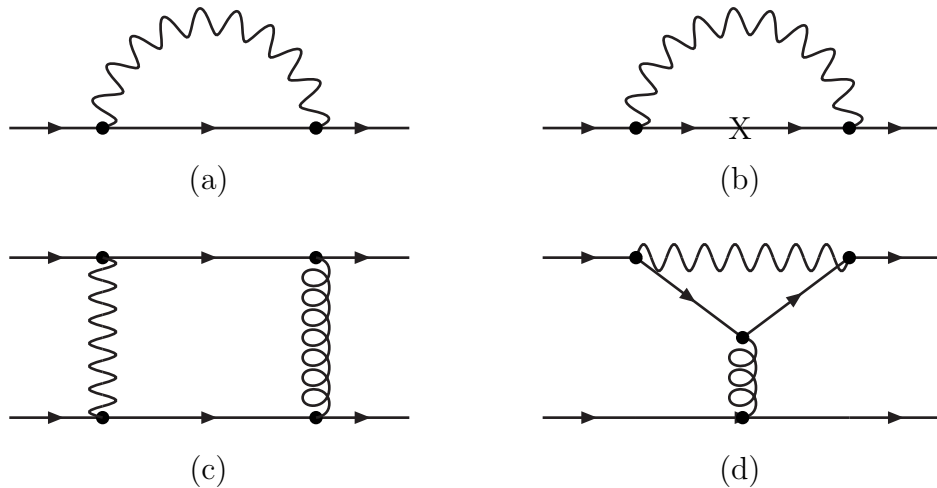


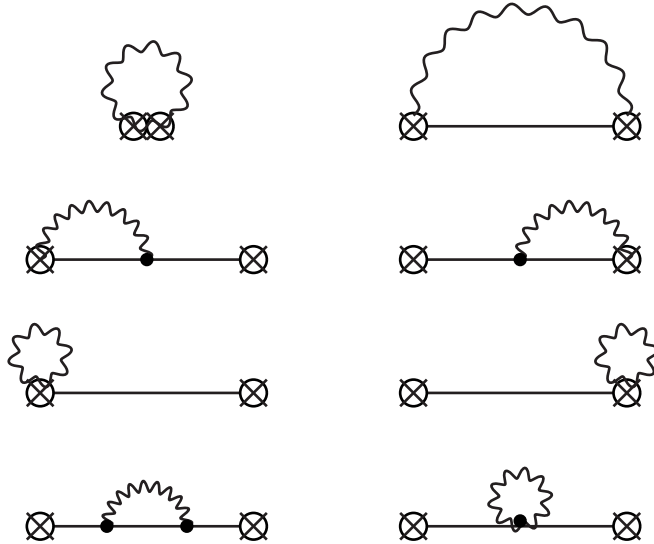
Figure 3: These are the four contributing diagrams. The curly line is the gluon, the wiggly the photon, the plain line the quark and the cross marks the external current.

In the leading order of $1/N_C$ ¹², Fig. 3c and Fig. 3d are just a product of pure QCD currents and their contributions have already been calculated in [1]. The other two diagrams have to do with the renormalization of the scalar, pseudo-scalar, vector and axial-vector currents, and the contribution depend on the

¹²The $1/N_C$ is a procedure where you assume the number of colours N_C to be large so that you can expand in $1/N_C$.

scale where the input current quark masses are renormalized in QED. This contribution has to some extent been calculated in [1], but in Ref.[12] by B. Moussallam it was pointed out that an extra contribution was needed. This implies a different SD result for the K_9 to K_{12} coefficients. We will use the result from [1] as much as possible in this text and just add the ChPT corrections of $\mathcal{O}(p^4)$ which originates from Fig. 3a and 3b.

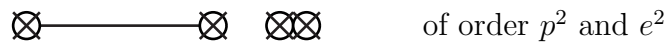
LD For this part we want to include all the orders in the QCD chiral Lagrangian expansion, so that a proper and a smooth result will appear and all the polynomial divergences will disappear. This is obviously not possible since there are an infinite number of orders. The expansion up to \mathcal{L}_6^{QCD} [14] is known, but *we will only consider \mathcal{L}_2^{QCD} and \mathcal{L}_4^{QCD}* . To this order the following relevant Feynman diagrams are generated:



The top left diagram might seem strange, but it just represents two external fields coupled to a photon loop. Thus it consist out of one vertex and a photon propagator.

Since we are only considering the leading and the next-to-leading order, problems will appear. For the LD part these problems can be avoided by using low energies, i.e. a small Λ which implies that terms like $L_i^2 \frac{\Lambda^4}{F_0^4}$, $L_i^3 \frac{\Lambda^6}{F_0^6}$, ... $\ll L_i \frac{\Lambda^2}{F_0^2}$. This means that to a good approximation for small momenta the higher order terms do not contribute.

Right hand side, (RHS) Here we have an effective Lagrangian in pure ChPT describing both QCD and QFD with internal photons. This means that ordinary field theory can be used. Since the tree level diagrams created by \mathcal{L}_2 are



the vertices of $\mathcal{O}(p^2)$ can be put together to one loop diagrams of order p^4 , e^2p^2 and p^0e^4 . These diagrams generate divergences of the same order, which can be removed by adding tree level diagrams from

$$\begin{array}{ccc}
 \otimes \text{---} \otimes & \otimes \otimes & \mathcal{L}_4 \text{ with } L_i \text{ of order } p^4 \\
 \otimes \text{---} \otimes & \otimes \otimes & \mathcal{L}_4 \text{ with } K_i \text{ of order } e^2p^2
 \end{array}$$

The L_i coefficients will absorb the p^4 divergence from the loop diagram created by \mathcal{L}_2 , and the K_i coefficients will remove the e^2p^2 divergence. *Since we are only interested in the K_i coefficients, the order that we are going to consider is e^2p^2 .* By renormalizing with dimensional regularization and \overline{MS} which is just a method to isolate the loop divergence and include some specific constant terms, all the infinities are absorbed into the LECs (the K_i and L_i coefficients in this case) and the Green function is well defined. When this renormalization is performed, a renormalization scale μ will appear just as in [7], this means that in the end the LECs will depend on this scale.

The resulting amplitudes from both sides are polynomials and logarithms of momenta, mass and electric charge. The identifications are done particle by particle combined with different external currents. Since the loop integrals are hard to calculate, simplifications, i.e putting $m_q = 0$ or $p^2 = 0$ on both sides helps the calculations. The one-loop diagrams will generate infrared (IR)¹³ divergences of the form $\log \frac{\Lambda^2}{-p^2}$, $\log \frac{\Lambda^2}{m^2}$ for the LHS and $\log \frac{\mu^2}{-p^2}$, $\log \frac{\mu^2}{m^2}$ for the RHS. As one can see this IR divergent part will cancel on both sides.

When both the SD and LD part on the LHS have been calculated and all the LECs of interest have been written in terms of Λ the two parts are plotted against each other, and compared to see at which region the result is approximately the same. In this way a reasonable region for the SD-LD separating scale Λ can be determined, and it can then be removed.

4 Result

In this section the result for all the calculations are presented:

From the two-point function, using ChPT in the external field formalism, the LD part and the RHS can be calculated. After matching the amplitudes on the two sides the following relations are obtained:

$$C = \frac{3 F_0^2 \Lambda^2}{2 16\pi^2} + \frac{3 L_{10}^r \Lambda^4}{16\pi^2} \quad (49)$$

¹³Just an other name for a something that go to infinity when the momentum goes to zero. The ultra violet (UV) divergences that show up in the SD contribution, goes to infinity when the momentum goes to infinity.

Achieved through: $\langle 0 | T(\pi^+(x)\pi^+(y)) | 0 \rangle$, using external pseudoscalar currents in the chiral limit to the $\mathcal{O}(p^0)$.

$$K_8^r = \frac{3}{8\pi^2} \frac{\Lambda^2}{F_0^2} (4L_6^r - L_4^r) - \frac{8C}{F_0^4} (2L_6^r - L_4^r) = \frac{3}{8\pi^2} \frac{\Lambda^2 L_4}{F_0^2} \quad (50)$$

Achieved through: $\langle 0 | T(\pi^+(x)\pi^+(y)) | 0 \rangle$, using external pseudoscalar currents with $p^2 = \hat{m} = 0$ to the $\mathcal{O}(p^2)$.

$$K_9^r - K_8^r = \frac{1}{128\pi^2} \left[(\xi - 1) \log\left(\frac{\Lambda^2}{\mu^2}\right) - \frac{3\Lambda^2}{F_0^2} (2L_4^r + L_5^r) \right] \quad (51)$$

Achieved through: $\langle 0 | T(\pi^+(x)\pi^+(y)) | 0 \rangle$, using external pseudoscalar currents with $p^2 = m_s = 0$ to the $\mathcal{O}(p^2)$.

$$\begin{aligned} K_9^r &= \frac{1}{128\pi^2} \left[(\xi - 1) \log\left(\frac{\Lambda^2}{\mu^2}\right) + \frac{3\Lambda^2}{F_0^2} (64L_6^r - 18L_4^r - L_5^r) \right] - \frac{8C}{F_0^4} (2L_6^r - L_4^r) \\ &= \frac{1}{128\pi^2} \left[(\xi - 1) \log\left(\frac{\Lambda^2}{\mu^2}\right) + \frac{3\Lambda^2}{F_0^2} (14L_4^r - L_5^r) \right] \end{aligned} \quad (52)$$

Achieved through: Eq. (50) and Eq. (51).

$$4K_{11}^r + (K_4^r - 2K_3^r) = \frac{1}{32\pi^2} \left[(\xi + 2) \log\left(\frac{\Lambda^2}{\mu^2}\right) + \frac{1}{2} - 12 \frac{\Lambda^2}{F_0^2} L_9^r \right] \quad (53)$$

Achieved through: $\langle 0 | T(\pi^+(x)\pi^+(y)) | 0 \rangle$, using external pseudoscalar currents in the chiral limit to the $\mathcal{O}(p^2)$.

$$2K_{12}^r - (K_4^r - 2K_3^r) = \frac{1}{32\pi^2} \left[-\log\left(\frac{\Lambda^2}{\mu^2}\right) + \xi \log\left(\frac{\Lambda^2}{\mu^2}\right) + 6 \frac{\Lambda^2}{F_0^2} L_9^r \right] \quad (54)$$

Achieved through: $\langle 0 | T(\pi^+(x)\pi^+(y)) | 0 \rangle$, using external axial-vector currents in the chiral limit to the $\mathcal{O}(p^2)$.

$$2K_{11}^r + K_{12}^r = \frac{1}{64\pi^2} \left[(1 + 2\xi) \log\left(\frac{\Lambda^2}{\mu^2}\right) + \frac{1}{2} - 6 \frac{\Lambda^2}{F_0^2} L_9^r \right] \quad (55)$$

Achieved through: Eq. (53) and Eq. (54)

$$\begin{aligned} -K_{13}^r + 2K_{14}^r + 4K_{12}^r - 2(K_4^r - 2K_3^r) &= \frac{1}{32\pi^2} \left[-2 \log\left(\frac{\Lambda^2}{\mu^2}\right) + \xi \left(\frac{-1}{4} + \frac{1}{2} \log\left(\frac{\Lambda^2}{\mu^2}\right) \right) + \right. \\ &\quad \left. + \frac{12\Lambda^2}{F_0^2} L_9^r + \frac{\Lambda^2}{F_0^2} (L_{10}^r - 2H_1^r) (12 - 3\xi) \right] \end{aligned} \quad (56)$$

Achieved through: $\langle 0 | T(\pi^+(x)\pi^+(y)) | 0 \rangle$, using external axial-vector currents in the chiral limit to the $\mathcal{O}(p^0)$.

$$\frac{2}{3}(K_5^r + K_6^r) = -(K_4^r - 2K_3^r) = -2(K_1^r + K_2^r) \quad (57)$$

$$K_7^r + K_8^r = 0 \quad (58)$$

$$K_9^r + K_{10}^r = 0 \quad (59)$$

In the calculation of the coefficients from the charged currents in Eq. (50) to Eq. (56) we have used the result from the neutral currents in Eq. (57) to Eq. (59). The observant reader has probably already noticed that some of the coefficients above are linear combinations of others. All together there exist 10 real combinations, the ones that are linear combinations are Eq. (52), Eq. (55) and Eq. (57). The reason why we display the linear combinations is that only certain combinations of the EM LECs have been calculated before, and to achieve those we need to rearrange our coefficients.

The processes that we used to calculate the coefficients above are not the only ones investigated, e.g. for the charge current we also investigated K^+ , but the combinations that came out of those calculations gave the same result as for the π^+ . For the neutral current we investigated contributions from η , π^0 , \bar{K}^0 and K^0 , which all contributed to the combinations in Eq. (57) to Eq. (59).

For the SD part which we calculated with perturbative QCD we got after comparing to the RHS:

$$C = \frac{3\alpha_s F_0^4 B_0^2}{8\pi \Lambda^2} \quad (60)$$

$$K_1^r = \frac{3\alpha_s F_0^2}{32\pi \Lambda^2} - \frac{2 L_4^r B_0^2}{3\pi \Lambda^2} \quad (61)$$

$$K_2^r = 0 \quad (62)$$

$$K_3^r = \frac{-3\alpha_s F_0^2}{32\pi \Lambda^2} \quad (63)$$

$$K_4^r = 0 \quad (64)$$

$$K_5^r = -\frac{\alpha_s F_0^2}{6\pi \Lambda^2} - \frac{\alpha_s L_5^r B_0^2}{3\pi \Lambda^2} \quad (65)$$

$$K_6^r = \frac{\alpha_s L_5^r B_0^2}{2\pi \Lambda^2} \quad (66)$$

$$K_7^r = \frac{-4\alpha_s L_6^r B_0^2}{3\pi \Lambda^2} \quad (67)$$

$$K_8^r = \frac{6\alpha_s L_6^r B_0^2}{\pi \Lambda^2} \quad (68)$$

$$K_9^r = \frac{-\alpha_s (2L_8^r + H_2^r) B_0^2}{6\pi \Lambda^2} - \frac{(1 - \xi)}{128\pi^2} \log \frac{\mu_0^2}{\Lambda^2} \quad (69)$$

$$K_{10}^r = \frac{3\alpha_s (2L_8^r + H_2^r) B_0^2}{4\pi \Lambda^2} + \frac{(4 - \xi)}{128\pi^2} \log \frac{\mu_0^2}{\Lambda^2} \quad (70)$$

$$K_{11}^r = \frac{3\alpha_s (2L_8^r - H_2^r) B_0^2}{4\pi \Lambda^2} - \frac{(4 - \xi)}{128\pi^2} \log \frac{\mu_0^2}{\Lambda^2} \quad (71)$$

$$K_{12}^r = \frac{(\xi - 1)}{64\pi^2} \log \frac{\mu_0^2}{\Lambda^2} \quad (72)$$

where the log contribution comes from Fig. 3a and Fig. 3b.

To be able to plot the SD part against the LD part, all the relevant coupling constants have to be known and the renormalization scales have to be chosen. All this is displayed in Tab. 4. As one might have noticed there are large errors in most of the parameters, and

Coefficient	fit 10	$\mathcal{O}(p^4)$	article		
$10^3 L_1^r$	0.43 ± 0.12	0.38	[3]		
$10^3 L_2^r$	0.73 ± 0.12	1.59	[3]		
$10^3 L_3^r$	-2.35 ± 0.12	-2.91	[3]		
$10^3 L_4^r$	0	0	[3]		
$10^3 L_5^r$	0.97 ± 0.11	1.46	[3]	$B_0 [GeV]$	1.63
$10^3 L_6^r$	0	0	[3]	α_s	0.3
$10^3 L_7^r$	-0.31 ± 0.14	-0.49	[3]	$\mu [GeV]$ (ChPT scale)	0.77
$10^3 L_8^r$	0.60 ± 0.18	1.00	[3]	$\mu_0 [GeV]$ (QCD scale)	1.0
$10^3 L_9^r$	5.93 ± 0.43	6.0	[2]		
$10^3 L_{10}^r$		-5.5	[6]		
$10^3 (2L_8^r + H_2^r)$		2.9 ± 1.0	[2]		
$10^3 H_1^r$		-4.1			
$F_0 [MeV]$	87.7	81.1	[3]		

Table 1: Displays the coupling constants that are needed to calculate the K_i s. The finite renormalized parts are at the scale $M_\rho = 0.77 GeV$. The values of the parameters to the left are all determined from articles. As one can see there are missing three fit 10 values. For these we use $\mathcal{O}(p^4)$ in both cases. The parameters to the right have values that we have chosen ourselves. B_0 are on the QCD scale $\sim 1 GeV$ and α_s is assumed to be constant. The ChPT parameter μ that appeared when we performed the dimensional regularization is chosen to be $\mu = M_\rho = 0.77 GeV$.

that will of course affect our result in the end. This is the reason why we have chosen two different fitting methods, fit 10^{14} and $\mathcal{O}(p^4)^{15}$, respectively, i.e. the change in the result in the end can be seen. This will of course affect some K_i^r constants more than others. In

¹⁴Include terms up to $\mathcal{O}(p^6)$, and is based on that L_4^r and L_6^r is equivalent to zero.

¹⁵Include terms up to $\mathcal{O}(p^4)$, and is based on that L_4^r and L_6^r is equivalent to zero

our calculations we also fix the gauge of the photon and use Feynman gauge, which means that the gauge fixing term ξ is put equal to zero.

All that remains now is to compare the LD with the SD, component by component, and that is done in Figs. 4 to Fig. 11. On the y-axis we have the value of the LEC and on the x-axis we have the cut-off Λ . The scale on the x-axis range from 0.3 GeV to 1.1 GeV , and the reason for this is that a Λ with a too high energy ($\sim 1 \text{ GeV}$) would disturb the perturbative treatment (can be seen from the figures where the higher order deviates faster for bigger Λ) and since our ChPT scale is around 1 GeV , it is not proper to exceed that energy. The reason why at low energies it does not work is that the perturbative expansion is not valid below $\sim 0.3 \text{ GeV}$.

The matching is done by finding the best region for LD4 and SD. This is done by looking at the region where the Sum4 function has the derivative closest to zero, but one also has to consider how the LD and SD parts behave. From Fig. 4 and Fig. 5 describing the coefficient C one can see how the next order (LD4) affects the result. If only the lowest order LD term were considered, the matching region would be easy to find. By adding the next order one can see that the matching region is not so good anymore, which means that the result would have a larger error. The difference between LD2 and LD4 is important, since in this text we are also interested in comparing the behavior of the two functions. As one can see there is no big difference between the fit 10 input and the $\mathcal{O}(p^4)$ input, that is why we only include the fit 10 graphs for the remaining quantities.

When K_8^r is calculated as in Fig. 6 the L_4^r and the L_6^r were put equal to 10^{-3} to avoid a non-zero result. In the figure we see that the sum of the LD and SD behaves nicely, which is good.

For K_9 in Fig. 7 both the sums behave nicely. The best matching region is a little too high, but it is still good enough. When we compare the two sums, we see that Sum4 is a little better.

For the $4K_{11}^r + (K_4^r - 2K_3^r)$ combination in Fig. 8 the Sum4 function behaves in an appealing way. The behavior of Sum2 is also rather good, the only thing to complain about is that the zero derivative area is a bit too low for Sum2 and a bit too high for Sum4. There is also a large difference between them.

Next we consider Fig. 9, Fig. 10 and Fig. 11 describing $2K_{12}^r - (K_4^r - 2K_3^r)$, $-K_{13}^r + 2K_{14}^r + 4K_{12} - 2(K_4^r - 2K_3^r)$ and $2K_{11}^r + K_{12}^r$, respectively. These graphs do not have a Sum4 that behaves as we want in the region of interest, but we still pick a Λ in our region, which means that the error in these parameters are big. For the $2K_{12}^r - (K_4^r - 2K_3^r)$ and $-K_{13}^r + 2K_{14}^r + 4K_{12} - 2(K_4^r - 2K_3^r)$ combinations one can also see that the Sum2 behaves much better.

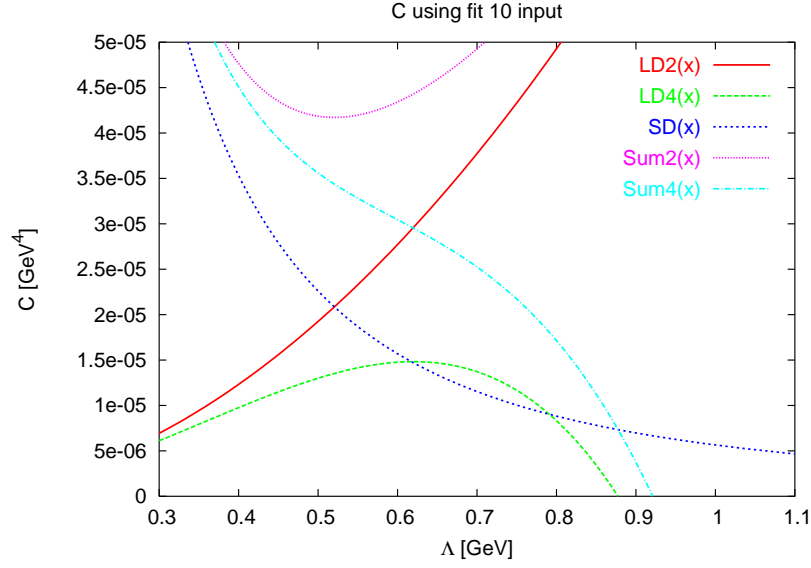


Figure 4: The long distance (LD), short distance (SD) and the sum as a function of the matching variable Λ for C . The number after the functions represents which $\mathcal{O}(p^n)$ that are considered. The fit 10 input parameters are used.

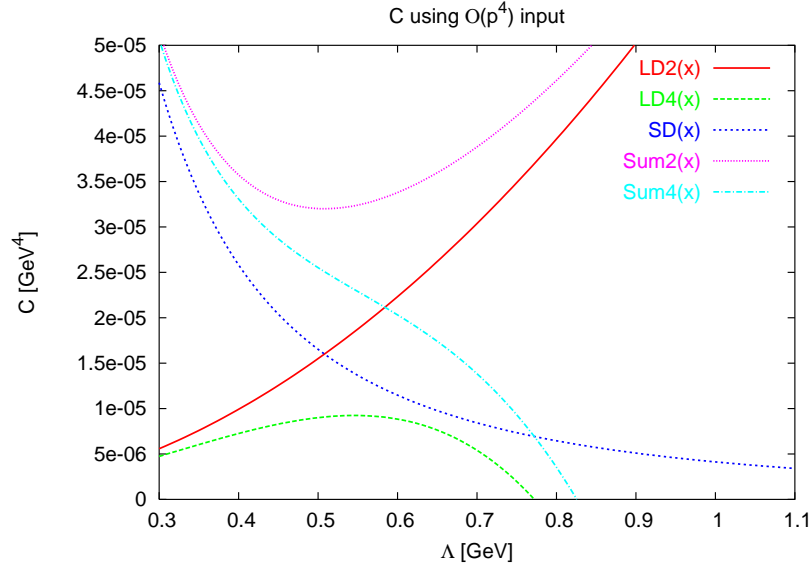


Figure 5: The long distance (LD), short distance (SD) and the sum as a function of the matching variable Λ for C . The number represents which $\mathcal{O}(p^n)$ that are considered. The $\mathcal{O}(p^4)$ input parameters are used.

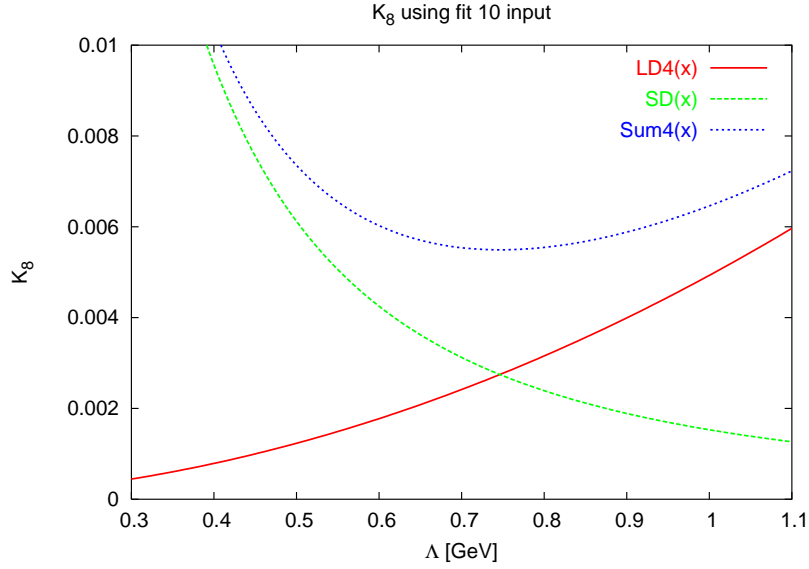


Figure 6: The long distance (LD), short distance (SD) and the sum as a function of the matching variable Λ for K_8^r . The number represents which $\mathcal{O}(p^n)$ that are considered. The fit 10 input parameters are used.

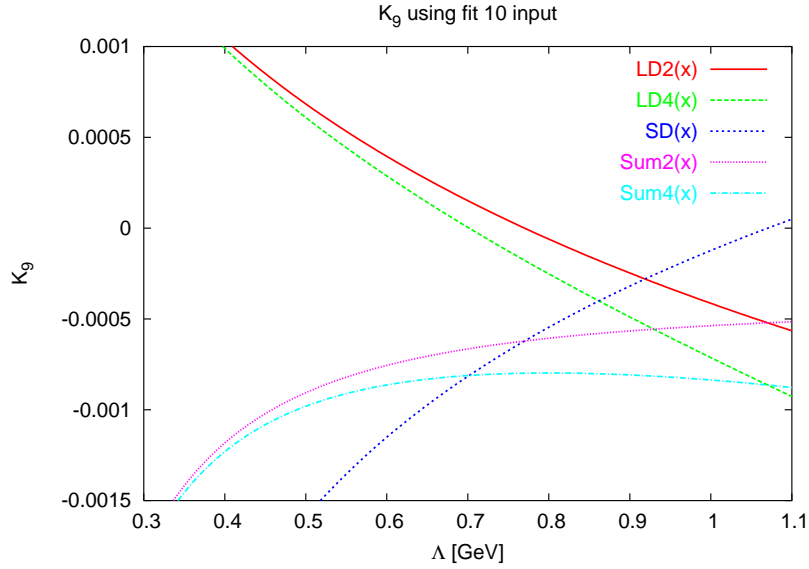


Figure 7: The long distance (LD), short distance (SD) and the sum as a function of the matching variable Λ for K_9^r . The number represents which $\mathcal{O}(p^n)$ that are considered. The fit 10 input parameters are used.

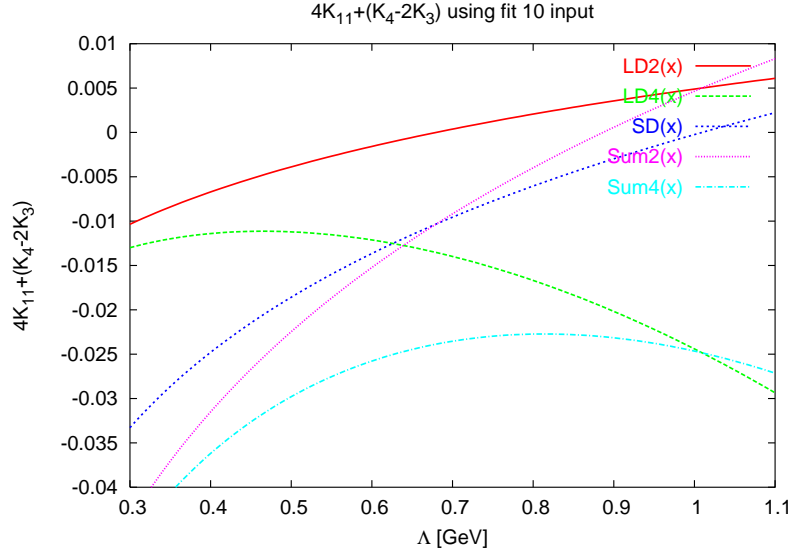


Figure 8: The long distance (LD), short distance (SD) and the sum as a function of the matching variable Λ for $4K_{11}^r + (K_4^r - 2K_3^r)$. The number after the functions represents which $\mathcal{O}(p^n)$ that are considered. The fit 10 input parameters are used.

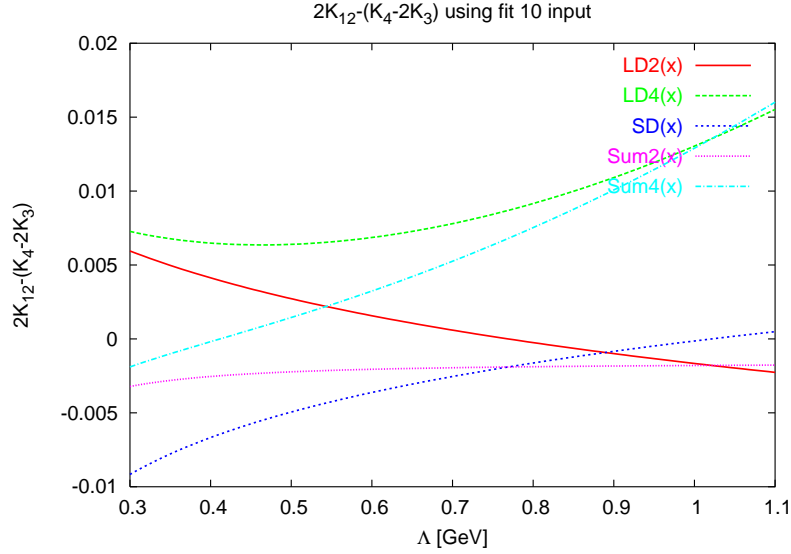


Figure 9: The long distance (LD), short distance (SD) and the sum as a function of the matching variable Λ for $2K_{12}^r - (K_4^r - 2K_3^r)$. The number after the functions represents which $\mathcal{O}(p^n)$ that are considered. The fit 10 input parameters are used.

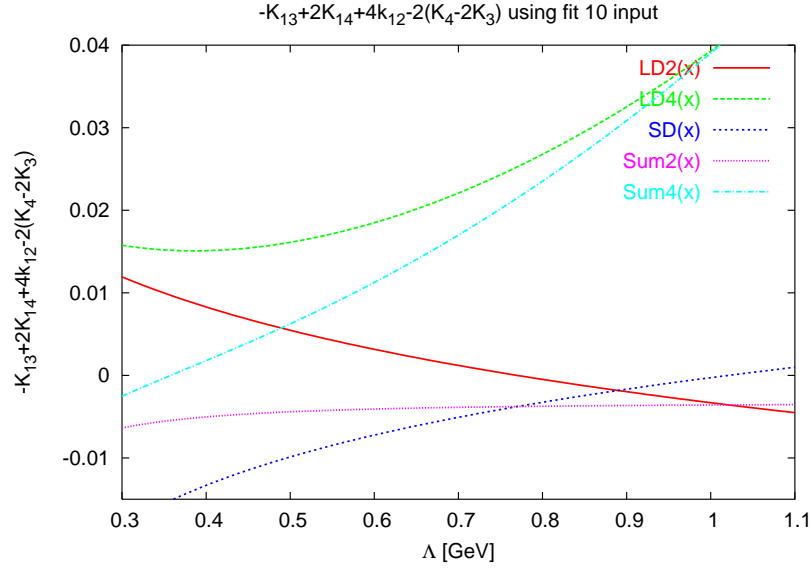


Figure 10: The long distance (LD), short distance (SD) and the sum as a function of the matching variable Λ for $K_{13}^r + 2K_{14} - 2(K_4^r - 2K_3^r)$. The number after the functions represents which $\mathcal{O}(p^n)$ that are considered. The fit 10 input parameters are used.

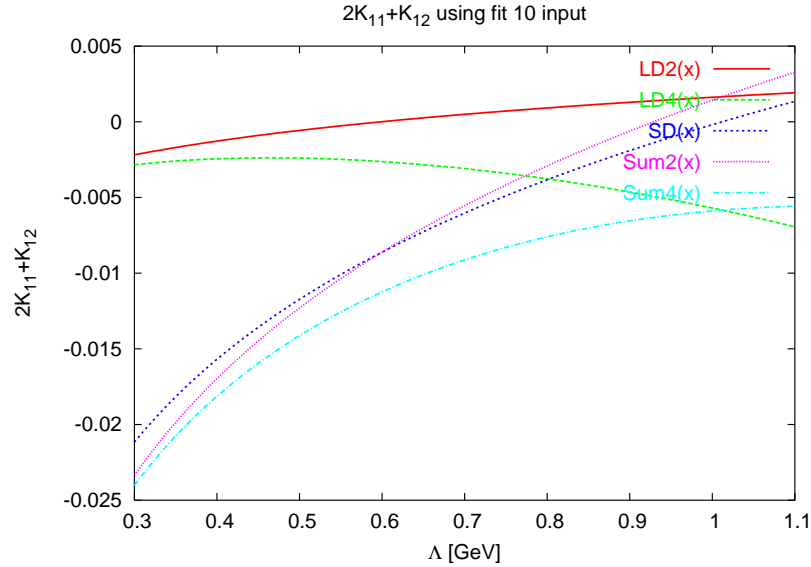


Figure 11: The long distance (LD), short distance (SD) and the sum as a function of the matching variable Λ for $2K_{11}^r + K_{12}$. The number after the functions represents which $\mathcal{O}(p^n)$ that are considered. The fit 10 input parameters are used.

The result from all the figures are summerized in the Tab. 2 below:

Table 2: The results for fit 10, “This work 1” is the value calculated in this text using fit 10, for “This work 2” we are using $\mathcal{O}(p^4)$. The Λ is value of the cut-off where the SD part best matches the LD part.

Coefficient	This work 1	Λ , fit 10 [GeV]	This work 2	Λ , $\mathcal{O}(p^4)$ [GeV]
C	3.0×10^{-5} [GeV ⁴]	0.62	2.25×10^{-5} [GeV ⁴]	0.58
K_8^r (used $L_4^r = L_6^r = 10^{-3}$)	5.8×10^{-3}	0.72	6×10^{-3}	0.71
K_9^r	-8×10^{-4}	0.8	-9×10^{-4}	0.73
$4K_{11}^r + (K_4^r - 2K_3^r)$	-2.3×10^{-2}	0.83	-2.3×10^{-2}	0.71
$2K_{12}^r - (K_4^r - 2K_3^r)$	4×10^{-3}	0.65	5×10^{-3}	0.65
$-K_{13}^r + 2K_{14}^r + 4K_{12} - 2(K_4^r - 2K_3^r)$	1.1×10^{-2}	0.6	1.4×10^{-2}	0.6
$2K_{11}^r + K_{12}^r$	-8×10^{-3}	0.8	-8×10^{-3}	0.8

Table 3: Displays the relevant calculated coefficients for each article. For [1] $F_0 = 89MeV$ was used, for [12] the improved Z value for K_9 and K_{10} was used. In all the calculation of the values we have used $\mu_0 = 1 GeV$, $M_V = \mu = M_\rho = 0.77 GeV$, $F_\pi = F_0 = 92.4 MeV$, $M_A = M_{a_1} = 1.23 GeV$ and leading N_C order.

Coefficient	[1]	[12]	[13]
C [GeV ⁴]	4.2×10^{-5}	2.36×10^{-5}	
K_8^r	0.8×10^{-3}	0	
K_9^r	-1.3×10^{-3}	-3.62×10^{-3}	
$4K_{11}^r + (K_4^r - 2K_3^r)$	-5.0×10^{-3}		
$2K_{12}^r - (K_4^r - 2K_3^r)$			
$-K_{13}^r + 2K_{14}^r + 4K_{12} - 2(K_4^r - 2K_3^r)$			
$2K_{11}^r + K_{12}^r$		-5×10^{-3}	-1.94×10^{-3}

The relevance of some of the results in Tab. 2 is now discussed.

When we compare the values for C in Tab. 2 with the values in the articles in Tab. 3, one can see that they are rather similar, which is good.

The value for K_8^r will not be discussed because of the arbitrary chosen L_i^r parameters.

Instead we turn to K_9^r which have a good matching region, and as we see these values are rather close to the one derived in [1].

The values for $4K_{11}^r + (K_4^r - 2K_3^r)$ are only calculated in [1], and they differ a lot compared to our values. Why is hard to say, but there are a lot of approximations that have been done in both cases.

For $2K_{12}^r - (K_4^r - 2K_3^r)$ and $-K_{13}^r + 2K_{14}^r + 4K_{12} - 2(K_4^r - 2K_3^r)$ no published values are accessible. So their values will not be commented further.

The last combination obtained is $2K_{11}^r + K_{12}^r$, which has values that are close to the value calculated in [12]. This means that our values are reasonable¹⁶, despite the large uncertainty.

In Tab. 2 one can see that the fit 10 and $\mathcal{O}(p^4)$ input do not differ much, which means that the largest error in the K_i^r coefficients are not due to the uncertainties in the L_i^r s, but instead due to the matching between the LD and SD parts.

5 Conclusion

In this thesis we have determined the renormalized and finite coefficients of the generating functional of ChPT up to $\mathcal{O}(p^4)$ including virtual photons to one-loop. The finite part incorporates 29 low energy coupling constants, and of those, 10 combinations of some the 14 K_i^r s have in the \overline{MS} scheme been written in terms of the experimentally known constants L_i^r , the cut-off Λ and the dimensional regularization parameter μ . The Λ dependences have been removed through the matching of the LD part to the SD part, which had a good match for some of the coefficients and a not so good for others. But over all the $\mathcal{O}(p^4)$ contribution made the result a little bit better. But the improvement is still not that big as we hoped it would be, which implies that the result of the naive leading order estimate in [11] is often good enough for a first estimate in the determination of the K_i constants. One could argue that a contribution of $\mathcal{O}(p^6)$ would improve this result, but it seems unlikely since higher orders tend to deviate more for Λ s in the upper region.

The determination of the effective low energy chiral Lagrangian is of great importance since it is used to determine the free quark mass difference $m_u - m_d$, which is not very well known. The procedure used, is based on that the physical $m_{K^+} - m_{K^0}$ mass difference has a pure QCD contribution due to the difference in quark masses and an electromagnetic contribution. Since the mass of the mesons can be determined experimentally, and quite accurate, then by calculating the EM contribution, the quark mass difference can be determined. This contribution can be calculated through different ChPT techniques, some better than others, often depending on region of interest. The procedure used by Bijnens-Prades in [1] includes all orders of p^2 in ChPT for the LD part, and this is done by using the ENJL model. Ananthanarayan-Moussallam in [12] and [13] also used a method where all orders of p^2 in ChPT were considered. The difference is that Moussallam used resonance saturation instead, but we will not explore the two methods more since it is beyond of the scope of this thesis.

One of the problems calculating the next-to-leading order electromagnetic coefficients is that the QCD coefficients are needed, the L_i^r s in this case. Most of these terms are not so well determined. In the near future, hopefully, these constants can be determined more

¹⁶To say that our value is reasonable, does not mean that it is the right value, since we do not really know which value that is the right one.

accurately.

Using the ChPT expansion on two-point functions as we did for the LD part, was not enough to determine all the LECs, as we were hoping. We even did the calculations for the four-point function for the K^0 (\bar{K}^0), but no new relation appeared. In the future one should investigate the four-point functions further and see if new K_i^r relations drop out.

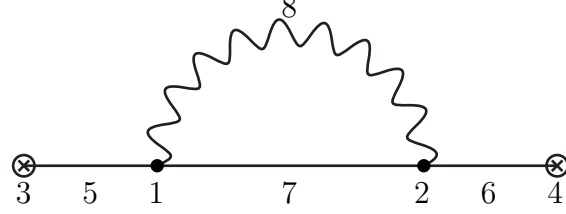


Figure 12: One of the basic Feynman diagrams for a two-point Green function.

A An easy example

Start by considering the leading-order effective QCD Lagrangian in Eq. (32). The U field in Eq. (33) and Eq. (34) is expanded in the following way:

$$\begin{aligned}
 U &= \exp\left(\frac{i\Phi}{F_0}\right) \simeq 1 + i\frac{\Phi}{F_0} - \frac{\Phi^2}{2F_0^2} + \dots \\
 U^\dagger &= \exp\left(\frac{i\Phi}{F_0}\right) \simeq 1 - i\frac{\Phi}{2F_0} - \frac{\Phi^2}{F_0^2} + \dots
 \end{aligned} \tag{73}$$

where $\Phi^\dagger = \Phi$ has been used. Taking the partial derivative of U in Eq. (73) yields

$$\begin{aligned}
 \partial_\mu U &= \frac{i}{F_0} \partial_\mu \Phi - \frac{1}{2F_0} (\partial_\mu \Phi \Phi + \Phi \partial_\mu \Phi) \\
 \partial_\mu U^\dagger &= -\frac{i}{F_0} \partial_\mu \Phi - \frac{1}{2F_0} (\partial_\mu \Phi \Phi + \Phi \partial_\mu \Phi).
 \end{aligned} \tag{74}$$

Putting Eq. (74) into the covariant derivative in Eq. (42) gives

$$\begin{aligned}
 D_\mu U &= \partial_\mu U - ieQA_\mu U + iUeQA_\mu = \\
 &= \frac{i}{F_0} \partial_\mu \Phi - \frac{1}{2F_0^2} (\partial_\mu \Phi \Phi + \Phi \partial_\mu \Phi) - ie[QA_\mu, \frac{i}{F_0} \Phi - \frac{\Phi^2}{F_0^2}] + \dots \\
 D_\mu^\dagger U &= -\frac{i}{F_0} \partial_\mu \Phi - \frac{1}{2F_0^2} (\partial_\mu \Phi \Phi + \Phi \partial_\mu \Phi) - ie[QA_\mu, \frac{i}{F_0} \Phi - \frac{\Phi^2}{F_0^2}] + \dots
 \end{aligned} \tag{75}$$

Now an expression for the first term in the Lagrangian in Eq. (32) has been derived and the Feynman diagram in Fig. 12 is ready to be evaluated.

1. Here a three vertex is investigated, where the only relevant terms from Eq. (32) are

the ones with one photon field A_μ , one Φ term and one $\partial_\mu\Phi$ term. So

$$\begin{aligned} \text{tr}(D_\mu U D^\mu U) &= \dots = \frac{-2eiA^\mu}{F_0^2} \text{tr}(\partial_\mu\Phi[Q, \Phi]) + \dots = \dots = \\ &\frac{-2eiA^\mu}{F_0^2} (-\partial_\mu\pi^+\pi^- - \partial_\mu K^+K^- + \partial_\mu\pi^-\pi^+ + \partial_\mu K^-K^+) + \dots \end{aligned} \quad (76)$$

This is interesting, since only π and K mesons showed up. Using ordinary Feynman rules and multiplying in the constants

$$\begin{aligned} A^\mu\partial_\mu\pi^-\pi^+ - A^\mu\partial_\mu\pi^+\pi^- &\rightarrow i(p_\mu^\pi + q_\mu^\pi) + ip_\mu^\pi \\ \implies \frac{F_0^2}{4} \frac{4ei}{F_0^2} (q_\mu^\pi + 2p_\mu^\pi) &= ei(q_\mu^\pi + 2p_\mu^\pi) \end{aligned} \quad (77)$$

$$\begin{aligned} A^\mu\partial_\mu K^-K^+ - A^\mu\partial_\mu K^+K^- &\rightarrow i(p_\mu^K + q_\mu^K) + ip_\mu^K \\ \implies ei(q_\mu^K + 2p_\mu^K). & \end{aligned} \quad (78)$$

2. The same as above, except that $\mu \rightarrow \nu$.
3. Here one external field couples to an interior. The second term in Eq. (32) contain the field couplings needed. The π^0, K^0 and η_8 is not considered since they did not show up in the three vertex. The resulting terms are then

$$\text{tr}(\chi U^\dagger + U \chi^\dagger) = i\sqrt{2}F_0B_0(P_{\pi^+}\pi^- + P_{K^+}\pi^-) + \dots \quad (79)$$

where

$$\begin{aligned} i\sqrt{2}F_0B_0P_{\pi^+}\pi^- &\rightarrow i\sqrt{2}F_0B_0 \\ i\sqrt{2}F_0B_0P_{K^+}\pi^- &\rightarrow i\sqrt{2}F_0B_0. \end{aligned} \quad (80)$$

4. The same result as above
5. In the propagator the derivative term squared and the mass term are of interest. So

$$\begin{aligned} \text{tr}\left(\frac{1}{F_0^2}(\partial_\mu\Phi)^2\right) + \text{tr}(\chi U^\dagger + U \chi^\dagger) &= \\ \frac{2}{F_0^2}(2\partial_\mu\pi^+\partial^\mu\pi^- + 2\partial_\mu K^+\partial^\mu K^-) - \frac{4B_0}{F_0^2}(2\hat{m}\pi^+\pi^- + \hat{m}K^+K^-) &+ \dots \end{aligned} \quad (81)$$

where $\hat{m} = (m_u + m_d)/2$. The complex fields above propagate in the following way

$$\begin{aligned} \partial_\mu\pi^+\partial^\mu\pi^- - 2B_0\hat{m}\pi^+\pi^- &\rightarrow \frac{i}{p_\pi^2 - 2B_0\hat{m}} \\ \partial_\mu K^+\partial^\mu K^- - B_0(\hat{m} + m_s)K^+K^- &\rightarrow \frac{i}{p_K^2 - B_0(\hat{m} + m_s)}. \end{aligned} \quad (82)$$

6. Achieve exactly the same terms as above

7. Here the resulting terms are

$$\frac{\frac{i}{(p_\pi + q_\pi)^2 - 2B_0\hat{m}}}{\frac{i}{(p_K + q_K)^2 - B_0(\hat{m} + m_s)}}. \quad (83)$$

8. This is the photon propagator, and only terms including $-\frac{1}{4}F_{\mu\nu}F^{\mu\nu} - \frac{1}{2(1-\xi)}(\partial_\mu A^\mu)^2$ are considered. The terms propagate according to

$$-\frac{1}{4}F_{\mu\nu}F^{\mu\nu} - \frac{1}{2(1-\xi)}(\partial_\mu A^\mu)^2 \rightarrow -i \int_0^\infty \frac{d^4q}{(2\pi)^4 q^2} (g_{\mu\nu} - \frac{\xi q_\mu q_\nu}{q^2}). \quad (84)$$

Adding all the parts for the Feynman diagram gives the following amplitudes for the π and K case, respectively:

$$\int_0^\infty \frac{d^4q}{(2\pi)^4} \frac{-2F_0^2 B_0^2 e^2 ((q_\pi + 2p_\pi)^2 - \xi \frac{[q \cdot (q_\pi + 2p_\pi)]^2}{q^2})}{(p_\pi^2 - 2B_0\hat{m})^2 ((p_\pi + q_\pi)^2 - 2B_0\hat{m})q^2} \\ \int_0^\infty \frac{d^4q}{(2\pi)^4} \frac{-2F_0^2 B_0^2 e^2 ((q_K + 2p_K)^2 - \xi \frac{[q \cdot (q_K + 2p_K)]^2}{q^2})}{(p_K^2 - B_0(\hat{m} + m_s))^2 ((p_K + q_K)^2 - B_0(\hat{m} + m_s))q^2}. \quad (85)$$

In the next step we calculate the one-loop integrals, where we integrate from zero to infinity. After transforming from Minkowski space to Euclidian space ($p^2 = (p^0)^2 - (\vec{p})^2 \rightarrow -p_E^2 = (p^0)^2 + (\vec{p})^2$) we can introduce a cut-off Λ and split the integral into two parts. The first part from zero to Λ gives us the following integral where the q independent terms are included in B

$$B \int_0^\Lambda \frac{d^4q}{(2\pi)^4} \frac{(q_\pi + 2p_\pi)^2 - \xi \frac{[q \cdot (q_\pi + 2p_\pi)]^2}{q^2}}{((p_\pi + q_\pi)^2 - 2B_0\hat{m})q^2}. \quad (86)$$

For the photons with a momentum greater than Λ you have to use other methods to calculate their contribution (see section 3). The important part is that in the end we want to compare the $p^2 e^2$ contribution from the effective QCD Lagrangian in Eq. (32) with the $p^2 e^2$ part of Eq. (44). This is done by putting e.g $m_q = 0$ or $p^2 = 0$ on both sides, i.e. the integrals are greatly simplified.

B Generating functionals

The two following sections are based on Ref. [15].

In this thesis Green functions in the form of two- respective four- point functions are used. They both originate from the matrix elements describing the physical process and the general matrix element is connected to a n -point function

$$\langle 0 | T(\phi(x_k) \cdots \phi(x_p)) | 0 \rangle = i^n \frac{\delta^n \ln W[j]}{\delta j(x_k) \cdots \delta j(x_p)} = G^{(n)}(x_1, \dots, x_n) \quad (87)$$

where $j(x)$ is the classical source field used to probe the theory, and it can be thought of as an external field. A physical picture of the above is shown in Fig. 13. The generating

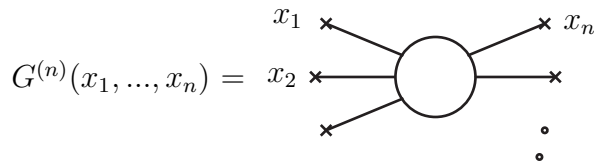


Figure 13: The figure shows n external fields coupled to some process.

functional W is associated with the sources in the following way

$$W[j] = \int [d\phi] e^{i \int d^4x (\mathcal{L}(\phi, \partial\phi) - j\phi)}. \quad (88)$$

and one should think of \mathcal{L} in Eq. (88) as describing physical processes inside the big bubble in Fig. 13 and the external fields as creating and annihilating particles on the edge of the bubble. So the bubble contain all relevant Feynman diagrams, e.g the ones in Fig. 2.

The two-point function is often written as a Fourier transform into momenta of the matrix elements with only two sources (four sources for a four point function). In the path integral formalism the two-point function can be written as

$$\Pi(q^2) = i \int d^4x e^{iqx} \langle 0 | T(P(0)P^\dagger(x)) | 0 \rangle \quad (89)$$

where $P(x)$ is a pseudoscalar source in our case.

C External fields

Here the idea about the external field formulation using generating functionals is presented. The external fields are a method that we use to be able to go from the generating functional to the Green function, and they can be thought of as the generalized j current of appendix B. One can also use the analogy where a particle is accelerated into a target particle and we investigate what comes out. The particle in this case is our external field and the target is the Green function.

The use of external fields has some advantages, i.e. it is independent of the G/H parameterization, allows for a well defined off-shell amplitude and it is obviously invariant

under chiral transformations. One more advantage is that the connection between QCD and the local properties become clearer.

The external fields are added to the Lagrangian and the generating functional can be written as

$$\begin{aligned}
e^{i\Gamma(v_\mu, a_\mu, s, p)} &\equiv \frac{1}{Z} \int [dq][dG] e^{i \int d^4x (\mathcal{L}_{QCD}^0 + \bar{q}\gamma^\mu (v_\mu + a_\mu \gamma_5) q - \bar{q}(s - ip\gamma_5)q)} \\
&\approx \frac{1}{Z} \int [dU] e^{i \int d^4x \mathcal{L}_{eff}(U, v_\mu, a_\mu, s, p)}
\end{aligned} \tag{90}$$

where the approximation is valid at low energies as we saw in the case of the non-linear sigma model. As seen in Eq. (90), the external currents contain quark currents and when the Lagrangians are differentiated with respect to the external field variables the pure quark current show up. The EM part could also be added to the Lagrangian above so that EM currents show up.

Acknowledgments

I would like to thank Johan ‘‘Hans’’ Bijmens for his valuable advises and for answering all my questions. The Master students at Vinterpalatset for their company at all the lunches and coffee breaks. And all the people that contributed with rewarding discussions, where a special thanks goes out to Timo Lahde.

References

- [1] J. Bijnens and J. Prades,
“Electromagnetic corrections for pions and kaons: masses and polarizabilities”
Nucl. Phys. B490, 239 (1997)
- [2] J. Bijnens and P. Talavera,
”Pion and Kaon Electromagnetic Form Factors”
JHEP 0203 (2002) 046
- [3] G. Amoros, J. Bijnens and P. Talavera,
”QCD isospin breaking in meson masses, decay constants and quark mass ratios”
Nucl. Phys B, B602 87-108 (2001)
- [4] S. Weinberg,
”Phenomenological Lagrangians”
Physica A96, 327 (1979)
- [5] J. Gasser and H. Leutwyler,
“Chiral perturbation theory to one loop” *Annals Phys.* 158, 142 (1984)
- [6] J. Gasser and H. Leutwyler,
”Chiral Perturbation Theory: Expansions in the mass of the strange quark”
Nucl. Phys. B250, 465 (1985)
- [7] R. Urech,
”Virtual photons in chiral perturbation theory”
Nucl. Phys. B433, 234 (1995)
- [8] G.’t Hooft,
“Renormalizable Lagrangians for massive Yang-Mills fields”
Nucl. Phys B 35, 167 (1971)
- [9] J. Goldstone,
“Field theories with ‘Superconductor’ solutions”
Nuovo Cim. 19, 154 (1961)
- [10] R. Dashen,
“Chiral $SU(3) \times SU(3)$ as a symmetry of the strong interactions” *Phys. Rev.* 183,
1245 (1969)
- [11] J. Bijnens,
“Violations of Dashen’s theorem”
Phys. Lett. B306, 343 (1993)

- [12] B. Moussallam,
“A sum rule approach to the violation of the Dashen’s theorem”
Nucl. Phys. B504, 381 (1997)
- [13] B. Ananthanarayan and B. Moussallam,
“Four-point correlator constraints on electromagnetic chiral parameters and resonance effective Lagrangians”
arXiv:hep-ph/0405206
- [14] J. Bijnens, G. Colangelo and G. Ecker,
“The mesonic chiral Lagrangian of order p^6 ”
JHEP 9902, 020 (1999)
- [15] Michael E. Peskin, Daniel V. Schroeder,
“An Introduction to Quantum Field Theory”
Westview press (1995), 661